

# Radiative Corrections to the Neutralino Dark Matter Relic Density - an Effective Coupling Approach

ARINDAM CHATTERJEE<sup>a,\*</sup>, MANUEL DREES<sup>a,b,†</sup> and SUCHITA KULKARNI<sup>c,‡</sup>

<sup>a</sup>*Physikalisches Institut and Bethe Center for Theoretical Physics,  
Universität Bonn, D-53115 Bonn, Germany*

<sup>b</sup>*KIAS, School of Physics, Seoul 130-722, Korea*

<sup>c</sup>*LPSC, 53 Av. des Martyrs, 38000, Grenoble, France*

## Abstract

In the framework of the minimal cosmological standard model, the  $\Lambda$ CDM model, the Dark Matter density is now known with an error of a few percent; this error is expected to shrink even further once PLANCK data are analyzed. Matching this precision by theoretical calculations implies that at least leading radiative corrections to the annihilation cross section of the dark matter particles have to be included. Here we compute one kind of large corrections in the context of the minimal supersymmetric extension of the Standard Model: corrections associated with two-point function corrections on chargino and neutralino (collectively denoted by  $\tilde{\chi}$ ) lines. These can be described by effective  $\tilde{\chi}$ -fermion-sfermion and  $\tilde{\chi}$ - $\tilde{\chi}$ -Higgs couplings. We also employ one-loop corrected  $\tilde{\chi}$  masses, using a recently developed version of the on-shell renormalization scheme. The resulting correction to the predicted Dark Matter density depends strongly on parameter space, but can easily reach 3%.

---

\*arindam@th.physik.uni-bonn.de

†drees@th.physik.uni-bonn.de

‡suchita.kulkarni@lpsc.in2p3.fr

# 1 Introduction

The presence of Dark Matter is by now well established. In fact, combining data from several cosmological observations, including in particular analyses of cosmic microwave background anisotropies, allows to determine the universally averaged Dark Matter density with an error of about 3% [1], assuming that the standard cosmological “ $\Lambda$ CDM” model, which combines a cosmological constant with essentially non-interacting cold Dark Matter, is correct. Note that this simple model describes all cosmological data satisfactorily. This error is expected to shrink to the 1% range once the PLANCK collaboration [2] releases their data.

A particularly attractive class of particle physics candidates for Dark Matter are Weakly Interacting Massive Particles (WIMPs). Their relic density can be calculated precisely in the framework of standard cosmology [3], assuming that the reheating temperature after inflation was higher than about 5% of the WIMP mass [4, 5, 6]. Input in this calculation is the WIMP annihilation cross section into Standard Model (SM) particles; the predicted relic density scales essentially like the inverse of this cross section. A precise prediction for the relic density therefore requires an accurate calculation of the total WIMP annihilation cross section.

This can only be accomplished within a specific WIMP model. Since the SM doesn’t contain a WIMP (nor any other plausible candidate for cold Dark Matter), it needs to be extended. The best motivated WIMPs are those that arise in extensions of the SM that have *independent* motivation, not related to Dark Matter.

Here we focus on supersymmetry, more specifically, on the minimal supersymmetric extension of the SM (MSSM) [7]. Superpartners of all SM particles not only stabilize the weak hierarchy against radiative corrections, they also allow single step Grand Unification of all gauge interactions. We assume that  $R$ -parity is exact, so that the lightest superparticle (LSP) is stable, thereby satisfying one of the conditions on a successful WIMP candidate. Moreover, we assume that the supersymmetry breaking terms conserve CP. Barring several finetunings, experimental constraints on CP violation, mainly from electric dipole moment measurements, require their phases to be small, unless superpartners of first (and second) generation fermions are very heavy [8, 9]. However, we do not assume a particular scenario for supersymmetry breaking (presumably described by high-scale dynamics), instead simply treating the relevant weak-scale soft breaking parameters as independent inputs.

The MSSM contains four potential WIMPs, the three sneutrinos  $\tilde{\nu}_i$  and the lightest neutralino  $\tilde{\chi}_1^0$ . However, sneutrinos have full weak strength vector couplings to the  $Z$ , leading to a cross section for scattering on protons that is well above experimental constraints, unless their masses are so large that their predicted relic density is well above the observed value. This leaves the lightest neutralino as unique WIMP candidate in the MSSM [10].

While there have been many analyses of  $\tilde{\chi}_1^0$  as WIMP candidate, nearly all of them compute the relevant annihilation cross sections only at tree level. However, in order to achieve percent level precision, at least the leading radiative corrections need to be taken into account. These include QCD corrections for strongly interacting final states [11, 12, 13, 14, 15], but at least leading electroweak corrections should also be included;

with “leading” we mean corrections that are parametrically larger than the naive one-loop factor  $\alpha/\pi$ .

Of course, a complete one-loop calculation would be ideal, and has in fact already been performed for a few points of parameter space [16, 17, 18]. However, calculating cross sections at one loop order involves computing a large number of diagrams. This not only needs a large effort even in the days of largely automatized calculation of one-loop amplitudes, the resulting expressions are also very complex, and their evaluation is very CPU intensive. With present-day computers the results of full one loop calculations can therefore not be used if the relic density has to be evaluated for many different choices of parameters.

It is therefore useful to develop alternative ways to estimate the bulk of electroweak radiative corrections to the relic density. One class of diagrams that can lead to large corrections involves the exchange of a relatively light boson between the annihilating WIMPs. These corrections can even become non-perturbative if the ratio of the boson and WIMP masses is smaller than the relevant squared coupling  $\alpha$  [19, 20, 21, 22], and they can remain significant even for larger mass of the exchanged boson. In the context of the MSSM these corrections are usually small [23], except in regions of parameter space where  $\tilde{\chi}_1^0$  is a heavy higgsino- or wino-like state [24, 25].

In this article we are interested in another class of potentially large radiative corrections, which can be described by running or effective couplings. For example, it has been recognized some time ago [11] that running quark masses, or Yukawa couplings, evaluated at a scale near  $m_{\tilde{\chi}_1^0}$ , should be used in the calculation of the  $\tilde{\chi}_1^0$  relic density. Similarly, most calculations of the  $\tilde{\chi}_1^0$  relic density employ running electroweak couplings, based on the QED coupling at the weak scale (often, at scale  $M_Z$ ), rather than the on-shell value of  $\alpha_{\text{em}}$ .

In the limit of exact supersymmetry these electroweak gauge couplings not only appear in  $\tilde{\chi}_1^0$  annihilation into final states containing gauge bosons, and in  $s$ -channel  $Z$ -exchange diagrams; they also determine the couplings of  $\tilde{\chi}_1^0$  to a Higgs boson and a neutralino or chargino, as well as the gauge contributions to the  $\tilde{\chi}_1^0$  couplings to a sfermion and a fermion, which have the structure of Yukawa couplings. However, when supersymmetry is broken, SM particles and their superpartners (for example,  $q$  and  $\tilde{q}$ ) no longer have the same masses, which leads to different contributions to gauge and gaugino two-point functions. In particular, for energies between the squark and quark mass scales, the (s)quark superfields no longer contribute to the running of the gauge Yukawa couplings, but the quarks still contribute to the running of the true gauge couplings. Corrections to the gauge Yukawa couplings are the supersymmetric analog of the oblique corrections, and have thus been dubbed “super-oblique” corrections [26, 27].<sup>§</sup>

While the first analyses of these super-oblique corrections only included terms that grow logarithmically with the masses of the heaviest superpartners [26, 29], references [30, 31] include the full quark and squark corrections to leptonic processes, thereby also including terms that approach a constant for large squark mass. Finally, in [32] this formalism was extended to include *all* (s)fermion loop corrections involving gauge Yukawa

---

<sup>§</sup>This apparent hard breaking of supersymmetry caused at one-loop order by soft breaking terms has first been noticed in the context of strong interactions in ref.[28].

couplings to the chargino and neutralino two-point functions. This allowed the introduction of effective neutralino and chargino couplings to sfermions and fermions; here we apply the same formalism also to the gauge Yukawa couplings involving a Higgs boson and two neutralinos or charginos.

Note that these corrections are enhanced not only by the logarithm of the ratio of the mass of the heaviest sparticle to the LSP mass, but also by the large number of fields contributing with the same sign (since the contributions to diagonal gaugino two-point functions go like the square of the relevant charge or coupling). The latter factor is more important, unless one is considering a scenario where some sfermions are more than an order of magnitude heavier than the LSP. A calculation [33] of radiative corrections to  $\tilde{\chi}_2^0 \rightarrow \tilde{\chi}_1^0 e^+ e^-$  decays found that the bulk of the corrections to the partial width could be described by these effective couplings even in a scenario where all superparticles are relatively light.

Since we include (certain) one-loop corrections to chargino and neutralino two-point functions, we also use one-loop renormalized neutralino and chargino masses. We use a recently developed [34] variant of the on-shell renormalization scheme [35], where corrections to physical masses are small for (nearly) all combinations of parameters, in contrast to earlier schemes, which lead to large corrections when the  $SU(2)$  gaugino and higgsino mass parameters become close in magnitude. The effect of this mass renormalization on the relic density is therefore usually (although not always) small.

This paper is organized as follows: in section 2 we outline our formalism and discuss the structure of the corrections included in the effective couplings. Section 3 contains technical details of our numerical calculation. Section 4 is devoted to the discussion of numerical results and we conclude in section 5. Details of the renormalization scheme we chose are given in the Appendices.

## 2 Formalism

In this section we describe the formalism of effective couplings, closely following [32], and discuss in some detail the nature of the corrections treated in this formalism. Here we are interested in corrections to the Yukawa couplings of the electroweak neutralinos and charginos. The required renormalization of the chargino, neutralino, Higgs and electroweak gauge sectors is described in the Appendices.

At tree level the neutralino and chargino couplings in question can be written as [32]

$$\begin{aligned} \mathcal{L}_{\tilde{\chi}_\alpha^0 \tilde{f} f} &= -\sqrt{2} g \tilde{\chi}_\alpha^0 \left[ T_3^f N_{\alpha 2}^* + \tan \theta_W \left( Q_f - T_3^f \right) P_L \tilde{f}_L^* - \tan \theta_W Q_f N_{\alpha 1} P_R \tilde{f}_R^* \right] f \\ &\quad - \frac{g m_f}{\sqrt{2} M_W f_f(\beta)} \tilde{\chi}_\alpha^0 \left[ N_{\alpha h_f}^* P_L \tilde{f}_R^* + N_{\alpha h_f} P_R \tilde{f}_L^* \right] f + h.c.; \end{aligned} \quad (1)$$

$$\begin{aligned} \mathcal{L}_{\tilde{\chi}_i^+ \tilde{d} u} &= -g \tilde{\chi}_i^+ U_{i1}^* P_L u \tilde{d}_L^* + \frac{g m_d}{\sqrt{2} M_W \cos \beta} \tilde{\chi}_i^+ U_{i2}^* P_L u \tilde{d}_R^* \\ &\quad + \frac{g m_u}{\sqrt{2} M_W \sin \beta} \tilde{\chi}_i^+ V_{i2} P_R u \tilde{d}_L^* + h.c.. \end{aligned} \quad (2)$$

The unitary  $4 \times 4$  matrix  $N$  appearing in eq.(1) diagonalizes the neutralino mass matrix, while the unitary  $2 \times 2$  matrices  $U, V$  appearing in eq.(2) diagonalize the chargino mass

matrix. Furthermore,  $g$  is the  $SU(2)$  gauge coupling,  $\theta_W$  is the weak mixing angle,  $T_3^f$  and  $Q_f$  are the third component of the weak isospin and electric charge of fermion  $f$ , respectively,  $P_{R,L} = (1 \pm \gamma_5)/2$  are the chiral projectors,  $m_f$  and  $M_W$  are the masses of fermion  $f$  and of the  $W$  boson, respectively, and  $\tan\beta$  is the ratio of vacuum expectation values (vevs) of the two neutral Higgs fields required in the MSSM. Finally, the function  $f_f(\beta)$  appearing in eq.(1) is  $\sin\beta$  for up-type quarks, and  $\cos\beta$  for down-type quarks and charged leptons; similarly, the index  $h_f = 4$  (3) for up-type quarks (down-type quarks and charged leptons). The chargino couplings to a neutrino and a charged slepton have the form of eq.(2) with  $u \rightarrow \nu$ ,  $\tilde{d} \rightarrow \tilde{\ell}$  (and  $m_u \rightarrow m_\nu = 0$  in our treatment). The chargino couplings to a down-type quark and an up-type squark again have the form of eq.(2), with  $u \leftrightarrow d$ ,  $U \leftrightarrow V$  and  $\tilde{\chi}_i^+ \leftrightarrow (\tilde{\chi}_i^+)^C$ , where the superscript  $C$  denotes charge conjugation.

Equations (1) and (2) have been written for neutralino and chargino mass eigenstates, but fermion and sfermion current eigenstates. In our numerical treatment we have ignored flavor mixing in both the fermion and sfermion sectors. Quark mixing is known to be quite small, and neutrino mixing is irrelevant for our purposes (since neutrinos remain very nearly degenerate and massless, compared to the sparticle masses). Moreover, sfermion flavor mixing is strongly constrained by experimental upper bounds on flavor changing neutral currents. However, in our numerical treatment we include  $\tilde{f}_L - \tilde{f}_R$  mixing for third generation sfermions.

Note that the first line in eq.(1) and the first term in eq.(2) come from gauge interactions, whereas the second line in eq.(1) as well as the second and third term in eq.(2), which are proportional to SM fermion masses, originate from superpotential couplings. Technically the corrections we are interested in originate from fermion–sfermion loop corrections to the chargino and neutralino two–point functions, plus the counterterms from (s)fermion loops needed to render them finite. Note that the sum of these explicit two–point function corrections and counterterms has to be finite, since these are the only one–loop corrections to  $\tilde{\chi}f\tilde{f}$  vertices involving (s)fermions  $f', \tilde{f}'$  of a *different*  $SU(2)$  multiplet. As usual, the finiteness of the results is an important check on the calculation.

In [32] all these contributions were absorbed in corrections to the matrices  $N$ ,  $U$  and  $V$ :

$$\tilde{U} = U + \Delta U, \quad \tilde{V} = V + \Delta V, \quad \tilde{N} = N + \Delta N. \quad (3)$$

Note that  $\Delta U$ ,  $\Delta V$ ,  $\Delta N$  are *not* counter terms; rather, they describe *finite* corrections to the *couplings* of charginos and neutralinos to sfermions and fermions, and to Higgs bosons.\* In our renormalization scheme, as in ref.[32], the mixing matrices are not renormalized at all, since we allow off–diagonal wave function renormalization counter terms.

---

\*A perhaps clearer, but bulkier, notation would be  $\Delta(gU)$ ,  $\Delta(gV)$ ,  $\Delta(gN)$ , which can be obtained from eqs.(4) by multiplying both sides with  $g$ ; note that even the contributions to the chargino and neutralino couplings (1) and (2) that originate from superpotential couplings have a factor of  $g$  in front. For easier comparison we here stick to the notation introduced by Guasch et al. [32].

Explicitly, the corrections defining the effective couplings are given by

$$\begin{aligned}
\Delta U_{i1} &= U_{i1} \left( \frac{\delta g}{g} + \frac{1}{2} \delta Z_i^{+R} \right) + U_{j1} \frac{1}{2} \delta Z_{ji}^{+R}, \\
\Delta U_{i2} &= U_{i2} \left( \frac{\delta g}{g} + \frac{1}{2} \delta Z_i^{+R} - \frac{1}{2} \frac{\delta M_W^2}{M_W^2} - \frac{\delta \cos \beta}{\cos \beta} \right) + U_{j2} \frac{1}{2} \delta Z_{ji}^{+R}, \\
\Delta V_{i1} &= V_{i1} \left( \frac{\delta g}{g} + \frac{1}{2} \delta Z_i^{+L} \right) + V_{j1} \frac{1}{2} \delta Z_{ji}^{+L}, \\
\Delta V_{i2} &= V_{i2} \left( \frac{\delta g}{g} + \frac{1}{2} \delta Z_i^{+L} - \frac{1}{2} \frac{\delta M_W^2}{M_W^2} - \frac{\delta \sin \beta}{\sin \beta} \right) + V_{j2} \frac{1}{2} \delta Z_{ji}^{+L}, \\
\Delta N_{\alpha 1} &= N_{\alpha 1} \left( \frac{\delta g}{g} + \frac{1}{2} \delta Z_\alpha^R + \frac{\delta \tan \theta_W}{\tan \theta_W} \right) + \sum_{\beta \neq \alpha} N_{\beta 1} \frac{1}{2} \delta Z_{\beta \alpha}^R, \\
\Delta N_{\alpha 2} &= N_{\alpha 2} \left( \frac{\delta g}{g} + \frac{1}{2} \delta Z_\alpha^R \right) + \sum_{\beta \neq \alpha} N_{\beta 2} \frac{1}{2} \delta Z_{\beta \alpha}^R, \\
\Delta N_{\alpha 3} &= N_{\alpha 3} \left( \frac{\delta g}{g} + \frac{1}{2} \delta Z_\alpha^R + \frac{1}{2} \frac{\delta M_W^2}{M_W^2} - \frac{\delta \cos \beta}{\cos \beta} \right) + \sum_{\beta \neq \alpha} N_{\beta 3} \frac{1}{2} \delta Z_{\beta \alpha}^R, \\
\Delta N_{\alpha 4} &= N_{\alpha 4} \left( \frac{\delta g}{g} + \frac{1}{2} \delta Z_\alpha^R + \frac{1}{2} \frac{\delta M_W^2}{M_W^2} - \frac{\delta \sin \beta}{\sin \beta} \right) + \sum_{\beta \neq \alpha} N_{\beta 4} \frac{1}{2} \delta Z_{\beta \alpha}^R. \tag{4}
\end{aligned}$$

In the first four equations, for  $\Delta U$  and  $\Delta V$ , the subscript  $j$  in the last term must always be different from  $i$  appearing on the left-hand sides, i.e. these are contributions from purely off-diagonal two-point functions, just like the corresponding contributions to the  $\Delta N$ . The counterterms  $\delta g$  and  $\delta \tan \theta_W$  are given in Appendix A, while  $\delta \sin \beta$  and  $\delta \cos \beta$  are given in Appendix C. Finally, the diagonal and off-diagonal wave function counterterms,  $\delta Z_i$  and  $\delta Z_{ij}$ , are given at the end of Appendix D; here the superscript  $L$  and  $R$  refer to chirality, while the superscript  $+$  refers to charginos.

We emphasize that  $\Delta N$ ,  $\Delta U$  and  $\Delta V$ , as described above, are process independent in the sense that they do not depend on the details of the external state [the flavor of the (s)fermion or the identity of the Higgs boson].

An important feature of these corrections is that heavy sparticles do *not* decouple; to the contrary, the size of the corrections *increases* logarithmically if some sfermions are much heavier than the charginos or neutralinos whose couplings are being computed. This observation is especially relevant in the light of recent LHC data which imply stringent lower bounds on the masses of first and second generation squarks, but allow relatively light superparticles with only electroweak interactions. As an illustration let us first review the origin of these non-decoupling effects only including gauge interactions.

Unbroken supersymmetry implies that the fermion-fermion-gauge boson (gauge) coupling  $g$  is the same as the corresponding sfermion-fermion-gaugino coupling  $\tilde{g}$ . Since supersymmetry is broken at a high scale (compared to the light fermion masses), the heavier sfermions *and fermions* will decouple from the running of  $\tilde{g}$  below the sfermion mass scale  $m_{\tilde{f}}$ . However, the corresponding fermion will still contribute to the running of  $g$ . Therefore,  $g$  and  $\tilde{g}$  “run apart” below the highest supersymmetry breaking scale.



We use the running coupling  $\alpha(M_Z)$  as tree-level input coupling, which is defined at the fixed scale  $M_Z$ . Consider a spectrum where sleptons, charginos and neutralinos have similar masses to each other, while squarks have much higher masses,  $m_{\tilde{\ell}} \sim m_{\tilde{\chi}} \ll m_{\tilde{q}}$ . We are interested in processes at the slepton or neutralino mass scale. On the other hand, full supersymmetry is attained only at scale  $m_{\tilde{q}}$ . Since between scales  $m_{\tilde{\chi}}$  and  $m_{\tilde{q}}$  the leptonic sector is still supersymmetric, leptons and sleptons contribute in the same way to the running of  $g$  and  $\tilde{g}$  in that range. Altogether we thus have:

$$\begin{aligned}
\tilde{g}(m_{\tilde{\chi}}) &= \tilde{g}(m_{\tilde{q}}) - \beta_{\ell, \tilde{\ell}} \log \frac{m_{\tilde{q}}}{m_{\tilde{\chi}}} \\
&= g(m_{\tilde{q}}) - \beta_{\ell, \tilde{\ell}} \log \frac{m_{\tilde{q}}}{m_{\tilde{\chi}}} \\
&= g(M_Z) + \beta_{\ell, q} \log \frac{m_{\tilde{\chi}}}{M_Z} + \beta_{\ell, q, \tilde{\ell}} \log \frac{m_{\tilde{q}}}{m_{\tilde{\chi}}} - \beta_{\ell, \tilde{\ell}} \log \frac{m_{\tilde{q}}}{m_{\tilde{\chi}}} \\
&= g(M_Z) + \beta_{\ell, q} \log \frac{m_{\tilde{\chi}}}{M_Z} + \beta_q \log \frac{m_{\tilde{q}}}{m_{\tilde{\chi}}} .
\end{aligned} \tag{5}$$

Here the particles contributing to the gauge beta function have been listed explicitly as subscripts; in the last step we have used the fact that to one-loop order the contributions of different (s)particles simply add up, i.e.  $\beta_{\ell, q, \tilde{\ell}} = \beta_{\ell, \tilde{\ell}} + \beta_q$ . Since SM fermions contribute with positive sign to the gauge beta functions, both logarithmic factors in the last line of eq.(5) are *positive* [26, 27].

We use on-shell renormalization both in the electroweak and in the  $\tilde{\chi}$  sector. Our effective  $\tilde{\chi}_i$  couplings can thus be understood as running couplings at scale  $m_{\tilde{\chi}_i}$ . This is the appropriate energy scale to describe  $\tilde{\chi}_i$  decays, where the effective couplings have been shown to reproduce the bulk of electroweak radiative corrections [33], as well as for the annihilation of two neutralinos, which is the main topic of the present investigation. It may not be the best choice for sfermion decays, where these couplings have first been introduced [32], nor for slepton production at a lepton collider via  $\tilde{\chi}$  exchange, where the  $\tilde{\chi}$  is always quite far off-shell.

The existence of Higgs superfields, whose superpotential couplings give rise to matter fermion masses and whose fermionic members mix with the gauginos, considerably complicates the picture. Fortunately the chirality structure allows to distinguish “gauge” and “superpotential” contributions to the  $\tilde{\chi} f \tilde{f}$  couplings: the former couple  $f_L$  to  $\tilde{f}_L$  and – for neutralinos coupling via hypercharge –  $f_R$  to  $\tilde{f}_R$ , whereas the latter couple  $f_L$  to  $\tilde{f}_R$  and  $f_R$  to  $\tilde{f}_L$ .

At one-loop level true Yukawa couplings  $\lambda$  do not renormalize true gauge couplings  $g$ . The above discussion of the  $\mathcal{O}(g^3)$  corrections to the “gauge” contribution of  $\tilde{\chi} f \tilde{f}$  couplings therefore indicates that there are *no*  $\mathcal{O}(g\lambda^2)$  corrections to these couplings. This is in fact true in the absence of gaugino–higgsino mixing, or, to good approximation, for gaugino–like states, where  $\mathcal{O}(g\lambda^2)$  corrections are suppressed by two factors of higgsino–gaugino mixing angles.

However, the “gauge” couplings of higgsino–like states do receive corrections  $\mathcal{O}(g\lambda^2)$ , where (s)top, (s)bottom and (s)tau loops all can contribute. These corrections are suppressed by one factor of a higgsino–gaugino mixing angle  $\epsilon$ ; however, since this is true already for this tree-level coupling, the relative size of the correction is not suppressed. Technically, these corrections involve the “vector” parts of diagonal as well as off-diagonal

$\tilde{\chi}$  two point functions, as well as the “scalar” parts of off-diagonal two-point functions; see eq.(26) for the decomposition of fermionic two-point functions. In the latter case, the product  $g\lambda_f m_f$  has been counted as  $\mathcal{O}(\lambda_f^2 \epsilon)$ , where the factor  $\epsilon$  describing suppression by higgsino–gaugino mixing arises from the combination of the factor  $M_W$  in  $m_f \propto \lambda_f M_W/g$  and the  $m_{\tilde{\chi}}$  factors in the expressions for the off-diagonal wave function counterterms given in eqs.(38) and (39).

Since there are no unsuppressed  $\mathcal{O}(g\lambda^2)$  corrections to the “gauge” couplings of gaugino-like states, these corrections cannot be understood in terms of running  $\tilde{g}$  couplings. Instead, in the framework of the effective theory defined by integrating out heavy sfermions, they can be interpreted as contributions to the running of those (off-diagonal) elements in the chargino and neutralino mass matrices that mix higgsino- and gaugino-like states.

This interpretation is supported by the observation that the “superpotential” couplings  $\tilde{\lambda}$  of gaugino-like states receive one-loop corrections  $\mathcal{O}(\lambda g^2)$ ,  $\mathcal{O}(\lambda^3)$ , where again all heavy (s)fermions contribute, that are only linearly suppressed by gaugino–higgsino mixing. Since these tree-level couplings suffer a similar suppression, the relative size of the corrections is again not suppressed. In contrast, the “superpotential” coupling of higgsino-like states only receives unsuppressed  $\mathcal{O}(\lambda^3)$  corrections, while  $\mathcal{O}(\lambda g^2)$  corrections are suppressed by *two* powers of higgsino–gaugino mixing angles; moreover, the for our application most relevant coupling  $\propto \tilde{\lambda}_\tau$  in this case does not receive unsuppressed corrections from the (s)top sector. This is consistent with the observation that only true Yukawa couplings contribute to the beta functions of other Yukawa couplings, if one restricts oneself to matter (s)fermion loops; since matter loops contribute with positive sign to the beta functions of superpotential couplings, the corresponding corrections are positive, just as in the pure gauge sector.<sup>†</sup>

Finally, the “gauge” couplings of higgsino-like states also receive  $\mathcal{O}(g^3)$  corrections, again suppressed by one factor of higgsino–gaugino mixing; these originate both from the running of the “gauge” coupling  $\tilde{g}$  and from  $\mathcal{O}(g^2)$  corrections to gaugino–higgsino mixing. Similarly, the “superpotential” couplings  $\tilde{\lambda}$  of gaugino-like states receive  $\mathcal{O}(\lambda^3)$  corrections, suppressed by one factor of higgsino–gaugino mixing, that can be understood from the running of  $\tilde{\lambda}$ .

Altogether, the tree-level and logarithmically enhanced  $\tilde{\chi}\ell\tilde{\ell}$  couplings, where  $\ell$  stands for a lepton, can be summarized by table 1, where we have not distinguished between  $g$  and  $\tilde{g}$ , nor between the superpotential coupling  $\lambda$  and the corresponding contribution  $\tilde{\lambda}$  to  $\tilde{\chi}f\tilde{f}$  couplings. Of course, our effective couplings also include terms that are not enhanced logarithmically for large sfermion mass. The corrections that vanish as some inverse power of the mass of the sfermion in the loop do not follow the pattern of this table; for example, there are  $\mathcal{O}(g\lambda_i^2 m_{\tilde{\chi}}^2/m_i^2)$  corrections to the “gauge” couplings of gaugino-like  $\tilde{\chi}$  states. However, these decoupling corrections are usually small in our numerical applications.

We repeat that the non-decoupling corrections from the gauge sector are enhanced by multiplicity factors in addition to possibly large logarithmic factors. Moreover, the

---

<sup>†</sup>In the full theory there are  $\mathcal{O}(g^2\lambda)$  corrections to the beta function of  $\lambda$ , but these are due to diagrams where members of gauge superfields run in the loop. These contributions cannot be included consistently into our effective couplings.



coupling	$\tilde{\chi} \simeq$ higgsino		$\tilde{\chi} \simeq$ gaugino	
	tree-level	one-loop	tree-level	one-loop
$\tilde{\chi}\ell_L\bar{\ell}_L, \tilde{\chi}\ell_R\bar{\ell}_R$	$\mathcal{O}(\epsilon g)$	$\mathcal{O}(\epsilon g^3, \epsilon g\lambda^2)$	$\mathcal{O}(g)$	$\mathcal{O}(g^3, \epsilon^2 g\lambda^2)$
$\tilde{\chi}\ell_L\bar{\ell}_R, \tilde{\chi}\ell_R\bar{\ell}_L$	$\mathcal{O}(\lambda_\ell)$	$\mathcal{O}(\lambda_\ell^3, \lambda_\ell\lambda_b^2, \epsilon^2\lambda_\ell g^2, \epsilon^2\lambda_\ell\lambda_t^2)$	$\mathcal{O}(\epsilon\lambda_\ell)$	$\mathcal{O}(\epsilon\lambda_\ell g^2, \epsilon\lambda_\ell\lambda^2)$

Table 1: Comparison of tree-level and one-loop contributions to slepton-lepton currents of different chiral structure, for higgsino- and gaugino-like charginos and neutralinos  $\tilde{\chi}$ . Here  $g$  stands for an electroweak gauge coupling,  $\lambda_\ell$  for the Yukawa coupling of lepton  $\ell$ , and  $\epsilon$  for one factor of gaugino-higgsino mixing, which is assumed to be small here. A coupling  $\lambda$  without subscript means that all superpotential couplings contribute without additional suppression. We do not distinguish between  $g$  and  $\tilde{g}$ , nor between  $\lambda$  and  $\tilde{\lambda}$ , in this table.

effective couplings capture all corrections  $\propto \lambda_\tau\lambda_b^2, \lambda_\tau\lambda_t^2$  to tree-level couplings  $\propto \lambda_\tau$ . They do, however, *not* capture all corrections  $\propto \lambda_t^3$  to tree-level couplings  $\propto \lambda_t$ ; since the latter also receive QCD corrections, which are also not included in our effective couplings, their application to  $\tilde{\chi}q\bar{q}$  couplings involving superpotential couplings is probably of limited usefulness.

As mentioned above, the corrections described by eqs.(4) can all be computed from two-point functions; see the Appendices for details. At a similar level of effort one can include corrections to the (pole) masses of the charginos and neutralinos. Of course, these are always computed from two-point functions only; we can, and do, therefore include the *complete* correction to the masses, including corrections from the gauge and Higgs sectors in addition to those from the matter (s)fermion sector.\* We do so using a recently introduced [34] variant of the on-shell scheme, where we consider the masses of the (more) wino-like chargino and of the (most) bino- and higgsino-like neutralinos as inputs, which are not altered by the corrections. In ref.[34] it was shown that the counterterms to  $M_1$ ,  $M_2$ , and  $\mu$  then remain well behaved in most of the parameter space, in contrast other versions of the on-shell scheme [35]. As a result  $\Delta N$ ,  $\Delta U$  and  $\Delta V$  also remain well behaved even when  $M_2 = |\mu|$ .

The expressions (4) were originally introduced [32] as corrections to couplings of charginos and neutralinos to fermions and sfermions. However, in addition, the corrections  $\Delta N_{\alpha 1}$ ,  $\Delta N_{\alpha 2}$ ,  $\Delta U_{i1}$  and  $\Delta V_{i1}$  can be used to (partly) absorb radiative corrections to all the vertices which involve a gaugino component of a chargino or neutralino but do *not* include a gauge boson. These include couplings of neutralinos and charginos to Higgs bosons, the *gaugino* component of which we also modify. However, the corrections  $\Delta N_{\alpha 3}$ ,  $\Delta N_{\alpha 4}$ ,  $\Delta U_{i2}$ ,  $\Delta V_{i2}$  should *not* be applied to these Higgs vertices, but *only* to vertices involving a (massive) fermion and one of its superpartners; as discussed above, part of the latter corrections can be understood as process independent corrections to chargino and neutralino couplings originating from the superpotential, whereas the couplings of

---

\*Computing the corrections to neutralino and chargino masses entails again computation of the counterterms  $\delta M_W$ ,  $\delta g$ ,  $\delta \cos\theta_W$  and  $\delta \cos\beta$ , now including *all* one-loop corrections. In the calculations of the one-loop corrected masses these counterterms will therefore have different numerical values than those appearing in eqs.(4), where *only* corrections from (s)fermion loops must be included in order to ensure finiteness of the effective couplings.

Higgs bosons to neutralinos and charginos are pure gauge couplings in the limit of exact supersymmetry.<sup>†</sup> Similarly, a vertex with a gauge boson involves a true gauge coupling. The running of the corresponding gauge coupling (the  $U(1)_Y$  and  $SU_L(2)$  gauge couplings in our context) takes care of all process independent radiative corrections to these vertices, which should therefore be written in terms of the *original*  $U$ ,  $V$ ,  $N$  matrices, *without* the corrections of eqs.(4).

Before presenting numerical results for corrections to neutralino annihilation cross sections, we wish to show some results for the corrections to neutralino couplings, i.e. the  $\Delta N_{\alpha\beta}$ . In Fig. 1 we plot the *relative* size of these corrections,  $\Delta N_{\alpha\beta}/N_{\alpha\beta}$ , for selected values of  $\alpha$  and  $\beta$ , against a common (i.e. generation and flavor independent) soft SUSY breaking sfermion mass  $M_{\text{SUSY}}$ . We assume the following parameters (all mass parameters are in GeV):

$$\tan\beta = 10, \quad M_A = 500, \quad M_1 = 100, \quad M_2 = 300, \quad M_3 = 1200, \quad \mu = 600, \quad A = 0. \quad (6)$$

Since  $\mu - M_{1,2} \gg M_Z$ , gaugino–higgsino mixing is suppressed, so the results of table 1 are applicable. Specifically,  $\tilde{\chi}_1^0$  is bino–like,  $\tilde{\chi}_2^0$  and  $\tilde{\chi}_1^\pm$  are wino–like, and  $\tilde{\chi}_3^0$ ,  $\tilde{\chi}_4^0$  and  $\tilde{\chi}_2^\pm$  are higgsino–like.

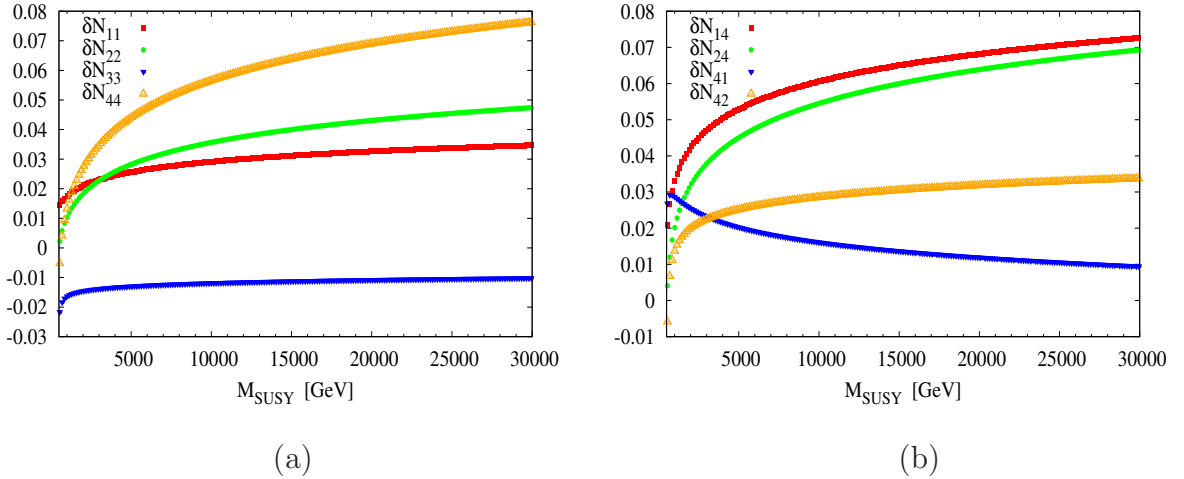


Figure 1:  $\delta N_{\alpha\beta} = \frac{\Delta N_{\alpha\beta}}{N_{\alpha\beta}}$ , as given by eq.(4) against  $M_{\text{SUSY}}$ , where  $M_{\text{SUSY}}$  denotes the common soft SUSY breaking sfermion mass.

The left frame shows corrections to couplings that are not suppressed by gaugino–higgsino mixing. Recall that the subscript  $\alpha$  in  $N_{\alpha\beta}$  refers to the mass eigenstate (ordered by increasing mass), while  $\beta = 1, 2, 3, 4$  refers to the bino, wino, down–higgsino and up–higgsino component, respectively. Clearly the biggest correction are those to  $N_{44}$ , which involve superpotential couplings of the “up–type” higgsino, in particular the top coupling  $\lambda_t$ . There are unsuppressed  $\mathcal{O}(\lambda_t^2)$  contributions to  $\delta N_{44}$ ; this case is analogous to the  $\mathcal{O}(\lambda_\ell^3)$  corrections to the  $\tilde{\chi}\ell_L\tilde{\ell}_R$  couplings in table 1. For the given, rather small, value

<sup>†</sup>Another way to see this is to note that it makes little sense to include higgsino two–point function corrections to a Higgs–higgsino–gaugino vertex, without including closely related two–point function corrections on the Higgs boson line.

of  $\tan\beta$ ,  $\delta N_{33}$  is far smaller, since it only receives contributions  $\propto \lambda_b^2, \lambda_\tau^2$ , plus  $\mathcal{O}(\epsilon^2)$  contributions. Not surprisingly, if  $\tan\beta \sim m_t/m_b$ ,  $\delta N_{33}$  is of similar size as  $\delta N_{44}$ .

Among the corrections to the dominant couplings of the gaugino-like neutralinos,  $\delta N_{22}$  increases significantly faster with increasing  $M_{\text{SUSY}}$  than  $\delta N_{11}$  does simply because the  $SU(2)$  gauge coupling is larger than the  $U(1)_Y$  coupling; this is only partly compensated by the fact that  $SU(2)$  singlet (s)fermions do contribute to  $\delta N_{11}$ .

The right frame of Fig. 1 shows corrections to couplings that are  $\mathcal{O}(\epsilon)$  at tree-level. The biggest corrections are to  $N_{14}$  and  $N_{24}$ , involving “superpotential” couplings of gaugino-like states. These corrections are dominated by  $\mathcal{O}(\lambda_t^2)$  running coupling effects, and are in fact of similar magnitude as  $\delta N_{44}$  shown in the left frame; recall that we are showing the *relative* size of the one-loop correction here, so that the  $\mathcal{O}(\epsilon)$  factor appearing in all couplings shown in the right frame cancel out.

The corrections to the “gauge” couplings of the higgsino-like states  $N_{41}$  and  $N_{42}$  are much smaller. These receive running coupling contributions proportional to the squared  $U(1)_Y$  and  $SU(2)$  gauge coupling, respectively, but are much smaller than  $\delta N_{11}$  and  $\delta N_{22}$  shown in the left frame. This indicates that the corrections to gaugino-higgsino mixing, which are dominated by  $\mathcal{O}(\lambda_t^2)$  contributions, tend to reduce the couplings in this case. In fact, the total coefficient of the correction  $\propto \log(M_{\text{SUSY}})$  to  $\delta N_{41}$  is negative. The fact that the overall correction nevertheless remains positive even at  $M_{\text{SUSY}} = 30$  TeV illustrates that the terms that approach constants for large sfermion masses can also be very important.

This completes our discussion of the effective couplings. Before presenting numerical results for the annihilation cross section and relic density of the lightest neutralino, we briefly describe the implementation of the effective couplings using publicly available software.

### 3 Implementation

In order to predict the relic density of the lightest neutralino at one-loop level, we have modified one of the publicly available codes for relic density calculation, **micrOMEGAs** (version 2.2.CPC.i) [36]. The algorithm describing the flow of relevant parameters is sketched in Fig. 2.

We use **SuSpect** [37] to compute the “tree-level” spectrum of superparticles and Higgs bosons. **SuSpect** actually includes various loop corrections in converting input  $\overline{\text{DR}}$  parameters into on-shell parameters and, hence, physical masses. However, in the neutralino-chargino sector these corrections are complete only in the absence of higgsino-gaugino mixing. Since we implement full one-loop corrections to all  $\tilde{\chi}$  masses in the on-shell scheme, we had to slightly modify [34] the  $\tilde{\chi}$  mass matrices used in **SuSpect**, using on-shell  $W$  and  $Z$  masses and the on-shell definition of the weak mixing angle  $\theta_W$ .

The output generated by **SuSpect** (in the format of the Supersymmetric Les Houches Accord, SLHA [38]) is used as input of **micrOMEGAs**. This program first computes two external libraries, written by us, which calculate the effective couplings and the renormalized masses, respectively. We have used **FeynArts**, **FormCalc** [39, 40, 41] and **LoopTools** [42] to compute the relevant diagrams and counterterms. Feynman gauge has been used

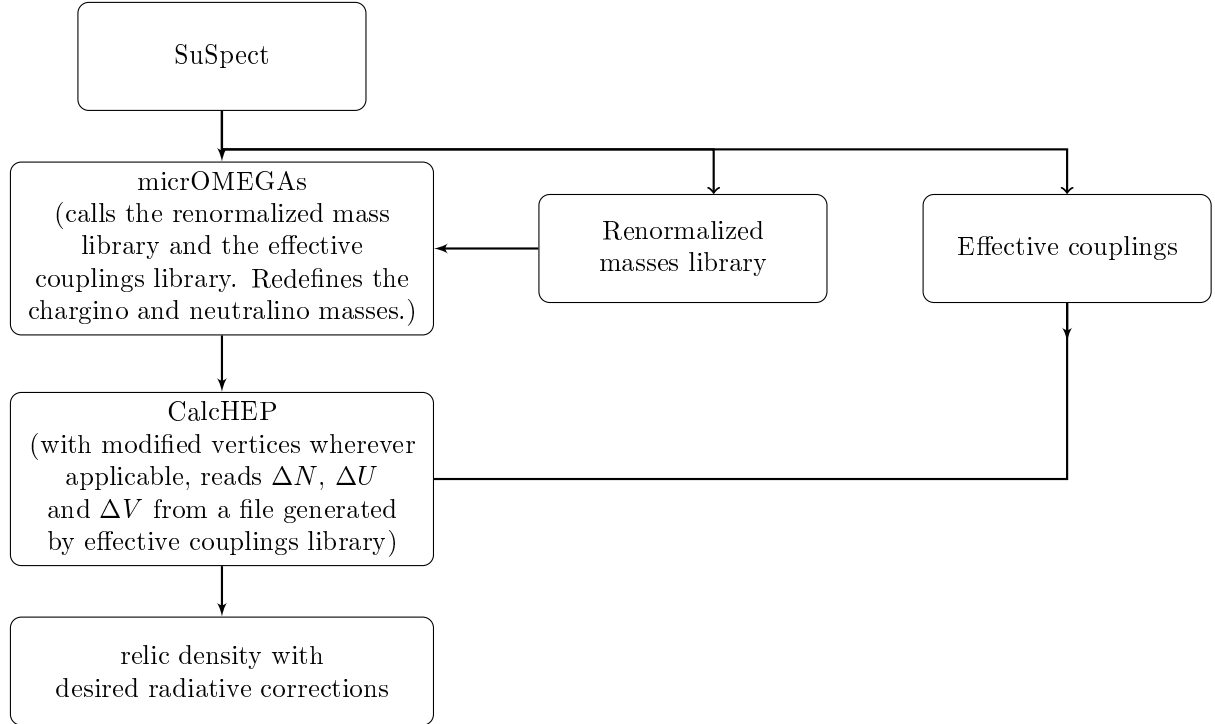


Figure 2: Flowchart describing the interaction of the publicly available codes **SuSpect** and **micrOMEGAs** with our subroutines calculating corrections to  $\tilde{\chi}$  masses and couplings.

in the calculation of one-loop corrections to  $\tilde{\chi}$  masses; the effective couplings do not include loops involving gauge bosons. For regularization we have used the constrained differential renormalization method [43]. At one-loop level this method has been proven to be equivalent [42] to regularization by the dimensional reduction method [44]. Note that, unlike the effective couplings, the renormalized masses involve contribution from all MSSM (s)particles; the two external libraries therefore use independent calculations of the relevant counterterms, as further described in the Appendices. In the loop diagrams, we for simplicity used running  $\overline{\text{DR}}$  sfermion masses defined at the electroweak scale, as given by **SuSpect**;<sup>\*</sup> the use of a different renormalization scheme for the sfermion masses inside the loops affects our results only at two-loop level. Moreover, we ignore  $L - R$  mixing for first and second generation sfermions, and do not include any flavor mixing.

**MicrOMEGAs** calculates the  $\tilde{\chi}_1^0$  (co-)annihilation cross sections with the help of **CalcHEP** [45]. We modified **CalcHEP** to read the effective couplings  $\Delta U$ ,  $\Delta V$  and  $\Delta N$ . These are used in *all*  $\tilde{\chi} f \tilde{f}$  couplings; the corrections to gaugino couplings  $\Delta U_{i1}$ ,  $\Delta V_{i1}$ ,  $\Delta N_{\alpha 1}$  and  $\Delta N_{\alpha 2}$  are also used in  $H \tilde{\chi} \tilde{\chi}$  vertices, but the corrections to higgsino couplings  $\Delta U_{i2}$ ,  $\Delta V_{i2}$ ,  $\Delta N_{\alpha 3}$  and  $\Delta N_{\alpha 4}$  are *not* used in these vertices, and the couplings between  $\tilde{\chi}$  states and gauge bosons are not modified at all.

We already mentioned that we use on-shell renormalization in the electroweak sector. This refers to the  $W$  and  $Z$  masses, the weak mixing angle  $\theta_W$  as well as the running electromagnetic coupling  $\alpha(M_Z)$ . For consistency we thus have to use on-shell

---

<sup>\*</sup>The reason is that the version of **SuSpect** we were using implemented certain  $\mathcal{O}(\lambda_t^2)$  corrections to stop masses, but not to sbottom masses, thereby creating spurious hard breaking of  $SU(2)$  in the stop-sbottom sector, with sizable effects on certain electroweak counterterms.

values for these quantities also in the tree-level calculation. This required additional changes of `micrOMEGAs`, which uses an on-shell  $M_Z$ , but the  $\overline{\text{MS}}$  value of  $\alpha(M_Z)$ , which is nearly 1% larger than the on-shell value, and an effective weak mixing angle such that  $\sin^2 \theta_W \simeq 0.231$  (compared to 0.222 in the on-shell scheme). We use this modified version of `micrOMEGAs` *only* for the one-loop corrected cross section. Since `micrOMEGAs` currently is the “industry standard” for calculations of the  $\tilde{\chi}_1^0$  relic density, we use its original version when evaluating the final corrections to the (co-)annihilation cross sections and relic density. The relative corrections to the annihilation cross sections are thus defined as

$$\delta\sigma = \frac{\sigma^{\text{tree, on-shell}} + \Delta\sigma^{1\text{-loop}} - \sigma^{\text{tree, orig}}}{\sigma^{\text{tree, orig}}}, \quad (7)$$

where  $\sigma^{\text{tree, orig}}$  is the prediction of the original version of `micrOMEGAs` using  $\overline{\text{MS}}$  values of  $\alpha(M_Z)$  and  $\theta_W$ .<sup>†</sup> We emphasize that using  $\sigma^{\text{tree, on-shell}}$ , computed with on-shell values for  $\theta_W$  and  $\alpha(M_Z)$ , as reference value would have led to significantly *larger* loop corrections  $\delta\sigma$  for bino-like  $\tilde{\chi}_1^0$ , largely because  $\alpha(M_Z)$  is smaller in the on-shell scheme, as mentioned above. Note finally that we use on-shell values of  $\alpha(M_Z)$  and  $\theta_W$  *only* in those vertices which we correct by the effective couplings. In all other vertices we continue to use `micrOMEGAs` default values of parameters; this includes all couplings of gauge bosons, as well as couplings of Higgs bosons to SM particles. This ensures that  $\delta\sigma$  defined in eq.(7) only shows effects of loop corrections we include but standard `micrOMEGAs` doesn’t include.<sup>‡</sup>

## 4 Numerical Results

Before presenting numerical results for a benchmark scenario, a qualitative discussion of the usefulness of the effective couplings for the calculation of the  $\tilde{\chi}_1^0$  relic density might be in order.

We expect the effective couplings to be most useful for dominantly bino-like neutralino [18]. A bino-like neutralino dominantly annihilates through  $t$  and  $u$  channel sfermion exchange to a pair of (lighter) fermions. Effective couplings absorb significant radiative corrections in both vertices. These will likely dominate the total electroweak corrections whenever squarks are significantly heavier than neutralinos and sleptons, since this leads to logarithmic enhancement of our corrections, as discussed above. The most important final states will then be  $\ell^+\ell^-$  pairs. Since the cross section is  $\propto |N_{11}|^4$ , the relative size of the correction can be estimated as  $4\delta N_{11}$ .

However, given existing lower bounds on slepton masses [46], pure slepton exchange usually gives too small an annihilation cross section, i.e. too large a  $\tilde{\chi}_1^0$  relic density (in standard cosmology). This can be corrected through co-annihilation with a slepton  $\tilde{\ell}$ , which also involves the  $\tilde{\chi}_1^0\ell\tilde{\ell}$  vertex.

---

<sup>†</sup>Recall, however, that we slightly changed the off-diagonal entries in the chargino and neutralino mass matrices in `SuSpect`; the resulting  $\tilde{\chi}$  masses and mixing angles are also used by the “original” `micrOMEGAs` in our calculation.

<sup>‡</sup>For example, changing  $\alpha(M_Z)$  and  $\theta_W$  everywhere would also lead to changes of the Higgs spectrum, which can lead to large changes of the annihilation cross section near Higgs poles; these would be entirely due to changes of input parameters, not due to radiative corrections.

The annihilation cross section of bino-like neutralinos can also be enhanced sufficiently (or even by too much) if there is a neutral Higgs boson with mass near twice the neutralino mass, the CP-odd state  $A$  being most efficient for this purpose. We also use an effective coupling for the gaugino components in the  $\tilde{\chi}\tilde{\chi}$  Higgs vertices. The flavor independent contributions to the two point function corrections to the gaugino components remain finite, and can absorb significant corrections to these processes.

Given lower bounds on chargino masses, higgsino- or wino-like neutralinos will annihilate dominantly into gauge boson pairs  $W^+W^-$ ,  $ZZ$ . These cross sections involve true gauge interactions, i.e. logarithmically enhanced loop corrections can be absorbed into the running of the  $SU(2)$  [and, in case of higgsinos,  $U(1)_Y$ ] gauge coupling. Our effective couplings can still capture leading corrections to subleading  $f\bar{f}$  final states for the annihilation of wino-like neutralinos; they are also likely to be quite important in the vicinity of possible  $s$ -channel Higgs resonances.

Let us now turn to a discussion of numerical results, based on the following benchmark scenario:

$$\begin{aligned} m_{\tilde{q}} &= 1.5 \text{ TeV}, M_3 = 1.2 \text{ TeV}, m_{\tilde{t}_L} = 0.55 \text{ TeV}, m_{\tilde{t}_R} = 0.50 \text{ TeV}, \\ \mu &= 0.6 \text{ TeV}, m_A = 0.5 \text{ TeV}, A_3 = 1.0 \text{ TeV}, \tan(\beta)(M_Z) = 10. \end{aligned} \quad (8)$$

All parameters except the on-shell mass  $m_A$  of the CP-odd Higgs boson are running  $\overline{\text{DR}}$  parameters, in most cases defined at the scale of electroweak symmetry breaking (EWSB), which in SuSpect is defined as  $\sqrt{m_{\tilde{t}_1}m_{\tilde{t}_2}} \simeq 1.5 \text{ TeV}$  in our benchmark scenario. This choice minimizes one-loop corrections to the effective potential for the neutral Higgs fields [47, 48]. Different values will be chosen for the  $SU(2)$  and  $U(1)_Y$  gaugino masses  $M_2$  and  $M_1$  in subsequent figures, as stated below.

The input value of  $\tan\beta$  is defined at scale  $M_Z$ , which is the SuSpect default. We have used  $\tan\beta^{\overline{\text{DR}}}$  at the EWSB scale, approximately equal to 9.6, for our calculations. We do not include any plots against  $\tan\beta$ , since neutralino masses and mixing matrices are not very sensitive to it.

In all parameter scans we ensure that  $\tilde{\chi}_1^0$  is the lightest supersymmetric particle. Since we assume exact  $R$  parity,  $\tilde{\chi}_1^0$  remains a dark matter candidate in these regions of parameter space. However, since the main goal of this paper is to show the relative size of the radiative corrections captured by effective couplings, we do not restrict ourselves to regions of parameter space giving the correct relic density in standard cosmology. Finally, in all figures showing  $\tilde{\chi}_1^0$  annihilation cross-sections, these have been calculated assuming the relative velocity between the annihilating neutralinos in their center of mass frame to be  $v = 0.3$ , which is typical for the epoch when the  $\tilde{\chi}_1^0$  decoupled from SM particles.

## 4.1 $M_1$ dependence

In Fig. 3a we plot  $\Delta N_{11}$ , the correction to the effective bino coupling of  $\tilde{\chi}_1^0$ , against  $M_1$ , for  $M_2 = 400 \text{ GeV}$ . Note that we show the total correction here, not the relative correction shown in Fig. 1. For  $M_1 < 410 \text{ GeV}$ ,  $\tilde{\chi}_1^0$  is bino-like and  $\Delta N_{11} \simeq 0.018$  is essentially independent of  $M_1$ . In this region of parameter space it is dominated by RG-like  $\mathcal{O}(g_Y^2)$  contributions, where  $g_Y$  is the  $U(1)_Y$  gauge coupling, and is thus positive. For  $M_1 > 410$



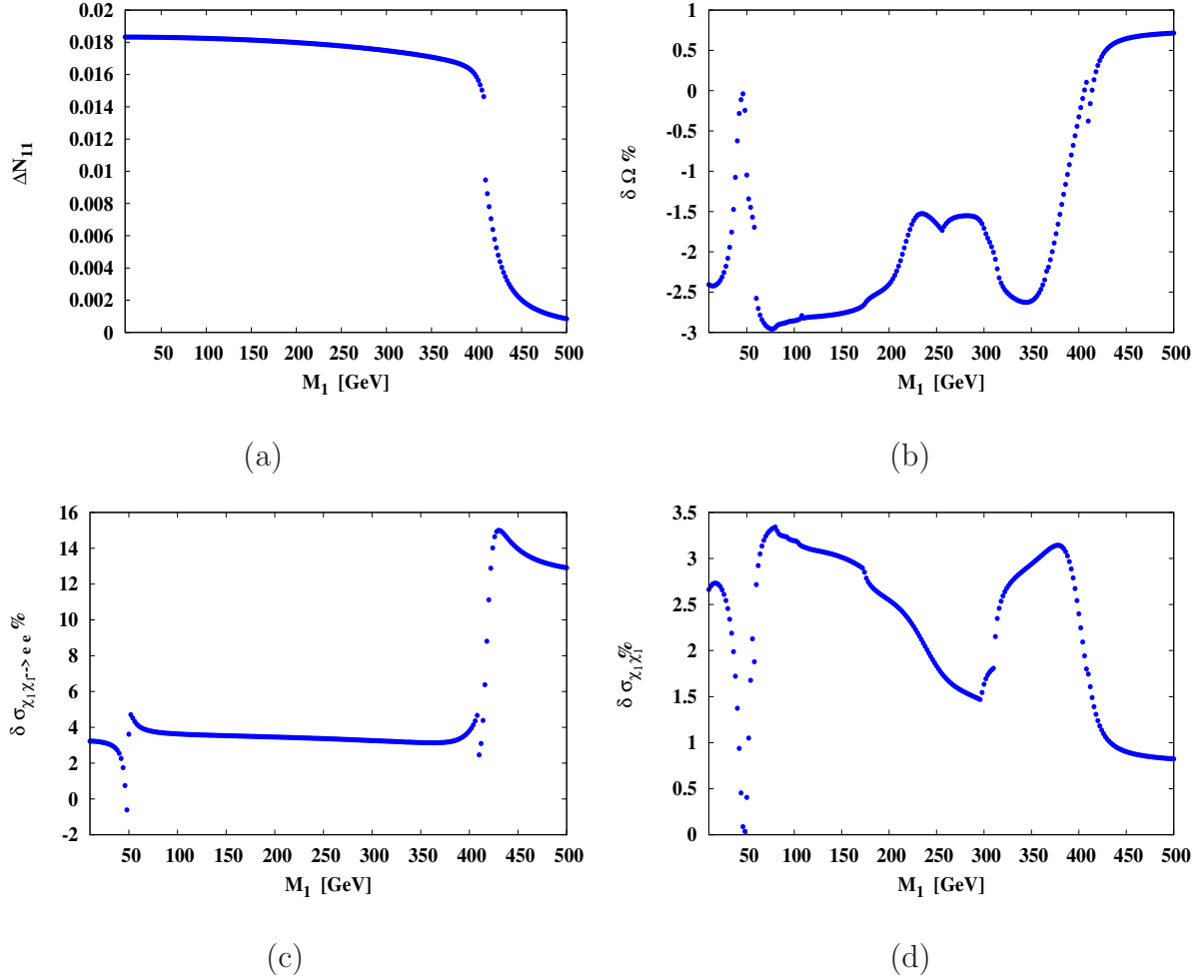


Figure 3: Effect of radiative corrections as function of the bino mass parameter  $M_1$  (in the  $\overline{\text{DR}}$  scheme at the electroweak symmetry breaking scale), for our benchmark point (8) with  $M_2 = 0.4$  TeV. We show the effective coupling  $N_{11}$  defined in eqs.(4) (top left); the relative correction to the predicted  $\tilde{\chi}_1^0$  relic density (top right); the relative correction to  $\sigma(\tilde{\chi}_1^0 \tilde{\chi}_1^0 \rightarrow e^+ e^-)$  (bottom left); and the relative correction to the total  $\tilde{\chi}_1^0$  annihilation cross section (bottom right). The last two plots are for fixed relative velocity  $v = 0.3$ . All relative corrections have been computed as in eq.(7).

GeV,  $\tilde{\chi}_1^0$  becomes wino-like. This has little influence on the relative size of the correction to the bino coupling, but, since  $|N_{11}|$  becomes much smaller than in the region of bino-like  $\tilde{\chi}_1^0$ ,  $\Delta N_{11}$  is also greatly reduced. Correspondingly, in this part of parameter space  $\Delta N_{11}$  no longer gives the most important correction to  $\tilde{\chi}_1^0$  annihilation.

The relative size of the correction to the  $\tilde{\chi}_1^0$  pair annihilation cross section into an  $e^+ e^-$  pair, defined as in eq.(7), is shown in Fig. 3c. Over most of parameter space this cross section receives its dominant contributions from selectron (in particular,  $\tilde{e}_R$ , due to the larger hypercharge) exchange in the  $t$ - and  $u$ -channels. For  $M_1 \leq 400$  GeV, where  $\tilde{\chi}_1^0$  is bino-like, the correction is then essentially given by  $4\Delta N_{11}$ ; the relative correction shown is smaller than this, because our reference cross section does not use on-shell values for  $\alpha(M_Z)$  and  $\theta_W$ , as explained in eq.(7). This indicates that it is indeed advantageous to

use the  $\overline{\text{MS}}$  value of  $\alpha(M_Z)$  if one is performing a tree-level calculation, since it reduces the size of the radiative corrections.\*

An exception occurs for  $M_1 \simeq 47$  GeV, where  $\tilde{\chi}_1^0$  annihilation can occur through the exchange of an almost on-shell  $Z$  boson. The very large enhancement factor  $(M_Z/\Gamma_Z)^2 \simeq 1300$  overcompensates the coupling suppression  $|N_{i3}|^2 - |N_{i4}|^2$  of this contribution to the matrix element. Since we do not modify the  $Z\tilde{\chi}_1^0\tilde{\chi}_1^0$  coupling, the size of the correction decreases at the  $Z$  pole.

As noted above, for  $M_1 \geq 410$  GeV  $\tilde{\chi}_1^0$  becomes wino-like. Here the corrections, which are now dominated by terms  $\propto \Delta N_{12}$ , become much larger; note that the cross section is now dominated by  $\tilde{e}_L$  exchange. We will see in Fig. 4a that  $|\delta N_{12}| \simeq 1.3\%$  increases the absolute size of the wino coupling, again due to RG-like effects. Moreover, recall that our tree-level calculation uses on-shell values of both  $\alpha(M_Z)$  and  $\theta_W$ . As a result, our tree-level  $SU(2)$  gauge coupling is about 1.5% larger than that used by `micrOMEGAs`. Altogether our  $\tilde{e}_L e \tilde{\chi}_1^0$  wino coupling is therefore about 3% larger than in `micrOMEGAs`, leading to an about 12% enhancement of the  $\tilde{\chi}_1^0$  annihilation cross section into  $e^+e^-$  pairs in the deep wino-like region. Note that for wino-like  $\tilde{\chi}_1^0$ , our choice of tree-level couplings leads to *smaller* radiative corrections than the choice made in `micrOMEGAs`. This is in contrast to experience with LEP observables, where the “effective” [49] or  $\overline{\text{MS}}$  [50]  $\theta_W^\dagger$  leads to smaller radiative corrections than the electroweak on-shell scheme. Recall, however, that for bino-like  $\tilde{\chi}_1^0$  the use of  $\overline{\text{MS}}$  values for  $\theta_W$  and  $\alpha(M_Z)$  reduces the size of radiative corrections.

The relative correction to the *total*  $\tilde{\chi}_1^0$  annihilation cross section, summed over all kinematically accessible final states, is shown in Fig. 3d. It exhibits a considerably more complicated dependence on  $M_1$  than the cross section for the  $e^+e^-$  final state does. The reason is that different final states become important for different ranges of  $M_1$ .

Near the  $Z$  pole the total annihilation cross section is again dominated by  $Z$  exchange, and the correction is small. For slightly larger  $M_1$ , the  $s$ -channel exchange of the lighter CP-even Higgs state  $h$  becomes (nearly) resonant. As noted earlier, we correct the gaugino component of the  $h\tilde{\chi}_1^0\tilde{\chi}_1^0$  coupling. Since the  $h$  exchange matrix element is linear in this coupling, the correction is considerably smaller here than in regions of parameter space where the total annihilation cross section is dominated by  $\tilde{\ell}$  exchange in the  $t$ - or  $u$ -channel. The correction therefore increases in size beyond the  $h$ -pole, reaching a maximum close to the relative size of the correction to the cross section for the  $e^+e^-$  final state at  $M_1 \simeq 80$  GeV.

At larger values of  $M_1$  additional channels begin to become accessible: annihilation into  $W^+W^-$ ,  $ZZ$ ,  $Zh$  and  $hh$  final states becomes possible at  $M_1 \simeq 84$  GeV, 94 GeV, 106 GeV and 118 GeV, respectively. Since the gauge vertices are not corrected and in many diagrams the Higgs vertex again only occurs linearly in the matrix element, the corrections begin to decrease; however, the total annihilation cross section is still dominated by  $\ell^+\ell^-$  final states.

---

\*The correction is further reduced because the small wino coupling of  $\tilde{\chi}_1^0$ , whose magnitude is also increased by the correction  $\Delta N_{12}$ , reduces the overall  $\tilde{e}_L e \tilde{\chi}_1^0$  coupling. However, this effect is numerically not very important, since the wino coupling remains very small, and the  $\tilde{e}_L$  exchange contribution is about 20 times smaller than the  $\tilde{e}_R$  exchange contribution; note that these contributions do not interfere in the limit  $m_e \rightarrow 0$ .

†These two definitions of the weak mixing angle differ conceptually, but are numerically very similar.

At  $M_1 \simeq 176$  GeV annihilation into  $t\bar{t}$  opens up. Since this cross section is not  $P$ -wave suppressed, it contributes significantly to the total annihilation cross section, although the relevant matrix element is suppressed either by the large stop masses (for the  $t$ - and  $u$ -channel diagrams) or the small  $\tilde{\chi}_1^0\tilde{\chi}_1^0$  Higgs couplings (for the  $s$ -channel Higgs exchange diagrams). The opening of this channel leads to a further reduction of the relative size of the corrections.

For yet larger values of  $M_1$ ,  $s$ -channel exchange of the heavy Higgs bosons  $H$  and  $A$  begins to dominate the total cross section. Since the corresponding matrix elements are again linear in the coupling we modify, the relative size of the corrections continues to decrease until, near  $M_1 = 300$  GeV, in rapid succession the  $H^\pm W^\mp$ ,  $ZA$ ,  $ZH$  and finally  $hA$  and  $hH$  final states become accessible. Many of these final states contribute significantly to the total annihilation cross section; note that, unlike  $hh$  and  $\ell^+\ell^-$  production,  $hA$  production is possible from an  $S$ -wave initial state, i.e. the cross section is not suppressed by a factor  $v^2 = 0.09$  in our calculation. Moreover, final states with two Higgs bosons can be produced via the exchange of higgsino-like states in the  $t$ - or  $u$ -channel; the corresponding diagrams are not suppressed by small couplings, and the suppression  $\mathcal{O}(M_1/\mu)$  by the heavy higgsino propagator is not very severe for  $M_1 \sim 300$  GeV. Since these diagrams involve two  $\tilde{\chi}\tilde{\chi}$  Higgs couplings, the relative size of the corrections begins to increase again for  $M_1 > 300$  GeV.

Finally, for  $M_1 \geq 410$  GeV the wino component of  $\tilde{\chi}_1^0$  begins to grow quickly. This leads to a rapid increase of the annihilation cross section into  $W^+W^-$  pairs, mostly via  $t$ - and  $u$ -channel  $\tilde{\chi}_1^+$  exchange diagrams. Since we do not modify any of the relevant couplings, the corrections quickly decrease, and remain very small once  $|N_{12}| \simeq 1$ .

The relative size of the correction to the predicted  $\tilde{\chi}_1^0$  relic density is shown in Fig. 3b. For  $M_1 \leq 350$  GeV it is essentially the mirror image of the correction to the total annihilation cross section, which we just discussed, because to good approximation the relic density is inversely proportional to the total annihilation cross section. There are some minor differences, because the evaluation of the relic density involves thermal averaging over a range of velocities, followed by integration over a range of temperatures, whereas the results of the cross section had been computed for a fixed relative  $\tilde{\chi}_1^0$  velocity, as mentioned above. As a result, the relative corrections to the relic density are slightly smaller in magnitude than those to the total annihilation cross section. This can be understood from the usual (semi-)analytical solution [51] of the Boltzmann equation determining the relic density. For a  $P$ -wave initial state, the relic density is inversely proportional to the product of the square of the decoupling temperature and the annihilation cross section. Our positive corrections increase the annihilation cross section, but also slightly decrease the decoupling temperature; because the latter depends only logarithmically on the annihilation cross section, the predicted relic density is indeed reduced, but by a slightly smaller amount than if the decoupling temperature was held fixed. The rapid change of the total annihilation cross section, and resulting change of decoupling temperature, also leads to a small kink at  $M_1 = 256$  GeV in the relative corrections to the relic density, right at the  $H, A$  exchange poles.

For  $M_1 \geq 350$  GeV, co-annihilation with the wino-like states  $\tilde{\chi}_2^0$  and  $\tilde{\chi}_1^\pm$  begins to be important. For  $M_1 > 410$  GeV,  $\tilde{\chi}_1^0$  itself is wino-like. A small discontinuity occurs at the cross-over value of  $M_1$ , since in our on-shell renormalization of the  $\tilde{\chi}$  sector the mass

of the most bino-like state is an input, i.e. is not corrected, while the mass of the most wino-like neutralino does receive (small) corrections. For  $M_1 > 410$  GeV we therefore not only correct certain  $\tilde{\chi}_1^0$  couplings, but also its mass.<sup>‡</sup>

In this region, co-annihilation with the (now bino-like)  $\tilde{\chi}_2^0$  no longer plays much of a role, but co-annihilation with  $\tilde{\chi}_1^\pm$  remains very important. This can lead to  $W^\pm Z$  final states, which are not affected by our corrections, as well as  $f\bar{f}'$  final states. The latter can be produced both via  $W^\pm$  exchange in the  $s$ -channel and by  $\tilde{f}, \tilde{f}'$  exchange in the  $t$ - or  $u$ -channel. Squark exchange diagrams are strongly suppressed by the large squark masses in our benchmark point. For leptonic final states we find strong cancellation between  $W$  and  $\tilde{\ell}$  exchange diagrams, which enhance the importance of the corrections to the  $\tilde{\chi}_1^0 \ell \tilde{\ell}$  as well as  $\tilde{\chi}_1^\pm \ell \tilde{\ell}'$  vertices. However, since most relevant (co-)annihilation cross sections are basically not sensitive to our corrections, the total size of the corrections to the  $\tilde{\chi}_1^0$  relic density remains below 1% here. Note that the correction to the relic density here has the same sign as the correction to the  $\tilde{\chi}_1^0$  annihilation cross section shown in Fig. 3d, since co-annihilation processes are more important than  $\tilde{\chi}_1^0 \tilde{\chi}_1^0$  annihilation reactions. Our corrections lead to an even more perfect cancellation between  $W^\pm$  and  $\tilde{\ell}$  exchange contributions to the production of leptonic final states in  $\tilde{\chi}_1^0 \tilde{\chi}_1^\pm$  co-annihilation, thereby slightly increasing the predicted  $\tilde{\chi}_1^0$  relic density.

Recall that all quantities in Fig. 3 are plotted against the  $\overline{\text{DR}}$  parameter  $M_1$ . The conversion of this, and other input  $\overline{\text{DR}}$  parameters in the chargino and neutralino mass matrices, into on-shell parameters made by **SuSpect** is exact only in the limit of vanishing mixing between the  $\tilde{\chi}$  states. According to ref.[52] this reproduces the exact on-shell masses quite accurately. This is consistent with our finding that one-loop corrections to  $\tilde{\chi}$  masses are small, at least in our version of the on-shell scheme. However, in the region of strong bino-wino mixing, where bino-wino co-annihilation is important, a small change of parameters in the  $\tilde{\chi}$  mass matrices can lead to relatively large changes of mixing angles. In particular, using running  $\overline{\text{DR}}$  values of  $M_W$ ,  $M_Z$  and  $\theta_W$  in the off-diagonal elements of the  $\tilde{\chi}$  mass matrices, as in the original **SuSpect**, leads to results for  $N_{12}$  and  $N_{22}$  which differ by up to 5% from those we obtain by using on-shell values of  $M_W$ ,  $M_Z$  and  $\theta_W$  everywhere, whereas the values of the  $\tilde{\chi}$  masses agree to within a fraction of a percent between the two calculations.

It might seem peculiar that the original **SuSpect** uses running, scale-dependent parameters in what are meant to be on-shell mass matrices. However, while on-shell masses are well defined as the poles of the (real parts of the) corresponding propagators, there is no correspondingly simple definition of a (non-diagonal) “on-shell mass *matrix*”. Indeed, we could have performed an on-shell renormalization of the  $\tilde{\chi}$  sector where the off-diagonal elements of the tree-level mass matrices were defined in terms of running  $M_W$ ,  $M_Z$  and  $\theta_W$ ; of course, (the finite parts of) certain counterterms would then differ from their values in our calculation. If one insists on using  $\overline{\text{DR}}$  input parameters, as in the supersymmetric Les Houches accord [38], the most consistent treatment is to use  $\overline{\text{DR}}$  renormalization throughout. On the other hand, if one insists on using on-shell renormalization, as we (and most other calculations of quantum corrections in supersymmetric theories) do, it seems more consistent to use the masses of the three input states as free parameters, rather than some  $\overline{\text{DR}}$  masses. If we compare results of our modified

---

<sup>‡</sup>The discontinuity in  $\Delta N_{11}$  shown in Fig. 3a has the same origin.

SuSpect with the original one for fixed values of the three input masses (e.g. of  $\tilde{\chi}_1^\pm$ ,  $\tilde{\chi}_1^0$  and  $\tilde{\chi}_3^0$  for  $M_1 \leq 410$  GeV), rather than for fixed  $M_1$ ,  $M_2$  and  $\mu$ , the two calculations also give very similar  $\tilde{\chi}$  gaugino components of the two lightest neutralinos.<sup>§</sup> This does not solve the problem of fixing the definition of on-shell mass matrices starting from  $\overline{\text{DR}}$  input parameters; this observation is nevertheless reassuring, since it indicates that the precise definition of the on-shell mass matrix may not matter very much once actual measurements are used to fix the parameters of the theory.

Finally, we mention that the  $\tilde{\chi}_1^0$  relic density attains the desired value  $\Omega_{\tilde{\chi}_1^0} h^2 \simeq 0.11$  for  $M_1 \simeq 230$  GeV,  $\simeq 265$  GeV (to either sides of the  $H, A$  poles) and  $\simeq 375$  GeV (where the wino component of  $\tilde{\chi}_1^0$  as well as co-annihilation with the wino-like states  $\tilde{\chi}_2^0$  and  $\tilde{\chi}_1^\pm$  become significant). For  $230 \text{ GeV} < M_1 < 265 \text{ GeV}$  as well as for  $M_1 > 380 \text{ GeV}$  the LSP could contribute a sub-dominant component of the overall cosmological Dark Matter.

## 4.2 $M_2$ dependence

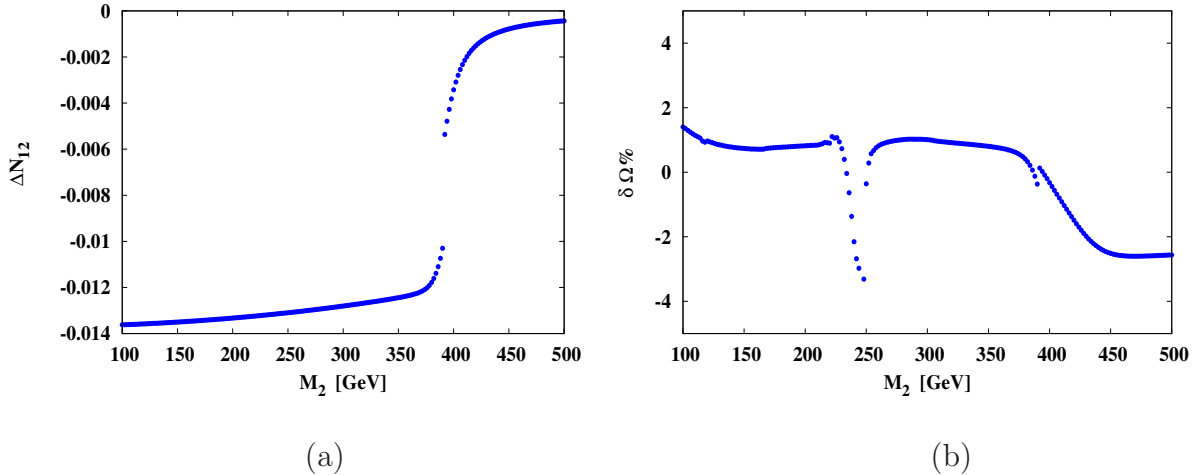


Figure 4: (a)  $\Delta N_{12}$ , as given by eq.(4) and (b) the relative size of radiative corrections to the relic density of  $\tilde{\chi}_1^0$ , as defined in eq.(7), against  $M_2$ , for our benchmark scenario (8) with  $M_1 = 400$  GeV.

In Fig. 4a, b we plot the dependence of the absolute correction to the wino coupling of  $\tilde{\chi}_1^0$  and the relative correction to the  $\tilde{\chi}_1^0$  relic density, respectively, on the wino mass parameter  $M_2$  for bino mass parameter  $M_1 = 400$  GeV. Note that  $N_{12} < 0$  here, i.e. the corrections increase the wino coupling  $|N_{12}|$ . The bulk of these corrections is RG-like, i.e. can be attributed to the running of the  $SU(2)$  component of the  $\tilde{\chi} f \tilde{f}$  “gauge” coupling. At first glance it might be surprising that the size of these  $\mathcal{O}(g^2)$  corrections is somewhat smaller than the  $\mathcal{O}(g_Y^2)$  correction shown in Fig. 3a, even though  $g^2 \simeq 3.3g_Y^2$ . The

<sup>§</sup>The higgsino components of these gaugino-like states, and the gaugino components of the higgsino-like states, still differ between these two tree-level calculations, but these have little effect on the relic density in this region of parameter space. Presumably these differences become very small if one compares one-loop calculations, since the two “tree-level” neutralino mass matrices only differ by  $\mathcal{O}(\alpha)$  terms.

reason for this is that in the on-shell scheme the wino coupling receives a sizable negative “constant” correction (which does not grow logarithmically with the sfermion masses): the rather small value of  $\sin^2 \theta_W \simeq 0.222$  leads to a tree-level  $SU(2)$  gauge coupling  $g = e/\sin \theta_W$  that is somewhat larger than the coupling used in standard `micrOMEGAs`, where  $\sin^2 \theta_W = 0.231$ . The total wino coupling  $g(N_{12} + \Delta N_{12})$  is independent of the choice of renormalization scheme.

Results for  $\Delta U_{11}$  and  $\Delta V_{11}$ , which describe the wino couplings of the lighter chargino, are very similar in magnitude to  $\Delta N_{12}$ ; these chargino couplings contribute to certain co-annihilation reactions.

At  $M_2 \sim 390$  GeV there is a discontinuity in  $\Delta N_{12}$ . This is because the dominantly wino-like neutralino no longer remains the lightest one, the bino-like one becomes the lightest state; we had found an analogous discontinuity in Fig. 3. As  $M_2$  is increased beyond this value,  $|\Delta N_{12}|$  quickly decreases, simply because  $|N_{12}|$  decreases as  $\tilde{\chi}_1^0$  becomes increasingly bino-like.

In most of the region with wino-like  $\tilde{\chi}_1^0$  that satisfies the LEP constraint  $M_2 \geq 110$  GeV [46] the corrections to the  $\tilde{\chi}_1^0$  relic density shown in Fig. 4b are quite small and positive. Here both  $\tilde{\chi}_1^0$  annihilation into  $W^+W^-$  pairs, and various  $\tilde{\chi}_1^0\tilde{\chi}_1^\pm$  co-annihilation reactions are important. As in Fig. 3b for  $M_1 > 400$  GeV, co-annihilation into leptonic final states is strongly suppressed by destructive interference between  $W^\pm$  and slepton exchange diagrams. The increase of the magnitude  $\tilde{\chi}_1^0$  and  $\tilde{\chi}_1^\pm$  couplings to  $SU(2)$  doublet (s)leptons further strengthens this cancellation; since this final state is in any case subdominant, the corrections increase the predicted relic density only slightly.

Within the region where  $\tilde{\chi}_1^0$  is wino-like, the corrections to the relic density become significant only in the vicinity of the  $s$ -channel  $A, H$  poles at  $M_2 \simeq 250$  GeV. The couplings of these Higgs bosons are essentially proportional to  $N_{12}$  here,  $N_{11}$  being very small. Since our corrections increase  $|N_{12}|$ , as noted above, they increase the Higgs exchange contributions to the annihilation cross section, and thereby reduce the relic density. Recall also that our tree-level  $SU(2)$  gauge coupling is about 1.5% larger than that used by `micrOMEGAs`; this also contributes to the corrections as defined in eq.(7). Note that there is also an  $H^\pm$  exchange pole in  $\tilde{\chi}_1^0\tilde{\chi}_1^\pm$  co-annihilation, which also contributes in this range of  $M_2$  since the masses of  $A, H$  and  $H^\pm$  are within a few hundred MeV of each other. Since, as noted above, the wino coupling of  $\tilde{\chi}_1^\pm$  is enhanced similarly as that of  $\tilde{\chi}_1^0$ , our corrections also enhance these contributions to the co-annihilation cross section. However, in both cases the Higgs couplings to  $\tilde{\chi}$  currents are suppressed by the small higgsino components of  $\tilde{\chi}_1^0$  and  $\tilde{\chi}_1^\pm$ ; hence Higgs exchange in the  $s$ -channel is important only for a narrow range of  $M_2$ .<sup>¶</sup>

Finally, for  $M_2 > 400$  GeV  $\tilde{\chi}_1^0$  becomes increasingly bino-like, as mentioned above. Here the corrections to the bino coupling,  $\Delta N_{11}$ , are of similar size as those shown in Fig. 3a for  $M_1 < 400$  GeV. In the transition region, co-annihilation with  $\tilde{\chi}_2^0$  and  $\tilde{\chi}_1^\pm$

---

<sup>¶</sup>Since a wino-like  $\tilde{\chi}_1^0$  isn't an input state in our on-shell renormalization of the  $\tilde{\chi}$  sector, its mass receives non-vanishing one-loop corrections in our calculation. However, they amount to less than 200 MeV in magnitude, significantly smaller than the total decay width of the heavy Higgs bosons, which amounts to  $\sim 1$  GeV in our benchmark scenario. These corrections to the  $\tilde{\chi}_1^0$  mass are therefore essentially irrelevant near the heavy Higgs poles, but lead to sizable changes of the relic density near the  $h$  pole; however, the lower bound on the  $\tilde{\chi}_1^\pm$  mass from LEP experiments [46] excludes the region of parameter space where a wino-like  $\tilde{\chi}_1^0$  has mass near  $m_h/2$ .



is important. For yet larger values of  $M_2$ , near the end of the range shown in Fig. 4, co-annihilation with these wino-like states is suppressed by the large bino-wino mass splitting, and annihilation into  $hA, ZH$  and leptonic final states dominates. Since our corrections increase the bino coupling of  $\tilde{\chi}_1^0$  by almost 2%, they increase many of the relevant cross sections, thereby reducing the predicted relic density by several percent.

In standard cosmology, the  $\tilde{\chi}_1^0$  relic density reaches its desired value for  $M_2 \simeq 425$  GeV, where  $\tilde{\chi}_1^0$  still has significant wino-component<sup>||</sup>, and co-annihilation with  $\tilde{\chi}_2^0$  and  $\tilde{\chi}_1^\pm$  is still significant. Our corrections reduce the relic density by about 2% at this point. For  $M_2 < 400$  GeV,  $\tilde{\chi}_1^0$  could only contribute less than 10% of the desired Dark Matter density.

### 4.3 $\mu$ dependence

Having discussed our corrections for bino- and wino-like  $\tilde{\chi}_1^0$ , we now consider a region of parameter space where  $\tilde{\chi}_1^0$  is higgsino-like, by fixing  $M_1 = 400$  GeV,  $M_2 = 600$  GeV and varying  $\mu$ , choosing  $\mu > 0$ . Note that there are two higgsino-like neutralinos. One of these states shows significantly stronger higgsino-gaugino mixing, which simultaneously reduces its higgsino content and its mass. Since the other, heavier higgsino-like state also has (even) larger higgsino content, its mass is one of the input masses in our version of the on-shell renormalization of the  $\tilde{\chi}$  sector. This means that the  $\tilde{\chi}_1^0$  mass does receive radiative corrections in our scheme, which can amount to several GeV. At the same time, the gaugino couplings of  $\tilde{\chi}_1^0$  receive corrections whose *relative* size is similar to those shown in figs. 3a and 4a for the bino- and wino-coupling, respectively; recall, however, that the bino- and wino-couplings of higgsino-like states also receive corrections that can be interpreted as corrections to the off-diagonal entries of the  $\tilde{\chi}$  mass matrices, rather than corrections that come from the running of the “gauge” couplings of the  $\tilde{\chi}$  states.

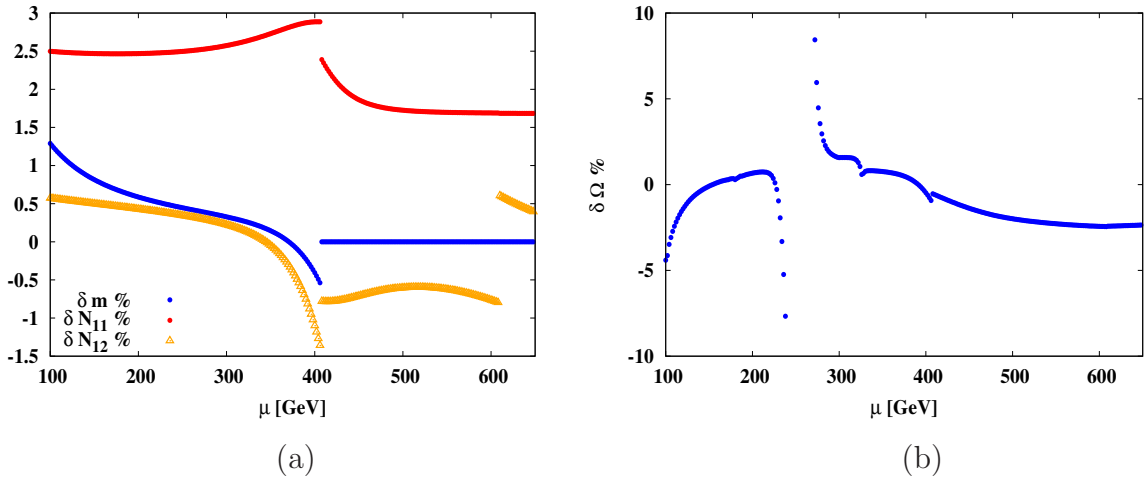


Figure 5: Relative size of the corrections to (a) the mass and gaugino couplings of  $\tilde{\chi}_1^0$ , and (b) to the predicted  $\tilde{\chi}_1^0$  relic density against  $\mu$ , for our benchmark point (8) with  $M_1 = 400$  GeV and  $M_2 = 600$  GeV.

<sup>||</sup>Of approximately equal size, but opposite sign, of a photino state.

In Fig. 5a we plot the relative size of the corrections to the mass and to the gaugino entries  $N_{11}$  and  $N_{12}$ . For  $\mu \leq 300$  GeV the absolute correction to the  $\tilde{\chi}_1^0$  mass is approximately 1.3 GeV, nearly independent of  $\mu$ , leading to a falling relative size of the correction with increasing  $\mu$ . For even larger values of  $\mu$  the bino-component of  $\tilde{\chi}_1^0$  begins to become sizable; this leads to a rapid decrease of the correction to the mass, which turns negative at  $\mu \simeq 370$  GeV. Note, however, that the correction remains small in magnitude even at  $\mu = M_1 = 400$  GeV, where other versions of the on-shell scheme are badly behaved [34]. For yet larger values of  $\mu$ ,  $\tilde{\chi}_1^0$  is bino-like; its mass is then an input, and does not receive any corrections.

Much of the correction to the relic density shown in Fig. 5b can be explained through this correction to the  $\tilde{\chi}_1^0$  mass. Note that higgsino-like neutralinos strongly (co-)annihilate into final states containing two gauge bosons;\* co-annihilation into  $f\bar{f}$  final states via  $s$ -channel exchange of a gauge boson is also important, while  $t$ - and  $u$ -channel sfermion exchange diagrams are suppressed by large sfermion masses (in case of squarks) and/or small Yukawa couplings of the corresponding fermions (in case of first and second generation sfermions). As a result, for most of parameter space none of these cross sections is affected significantly by our corrections to  $\tilde{\chi}_1^0$  couplings.†

The total correction to the relic density can nevertheless be sizable. This is most obvious in the vicinity of the heavy Higgs poles, where the positive shift of the  $\tilde{\chi}_1^0$  mass is important, since it slightly exceeds the width of the heavy Higgs bosons. It therefore significantly increases the cross section below the resonance, where the correction reduces the mass gap to the resonance, but reduces it above the resonance, where the corrections move  $\tilde{\chi}_1^0$  further away from the resonance. The positive correction to the  $\tilde{\chi}_1^0$  mass also increases the annihilation cross section for rather light  $\tilde{\chi}_1^0$ , close to the  $W^+W^-$  and  $ZZ$  thresholds where the corresponding cross sections are still significantly phase space suppressed. On the other hand, away from poles and thresholds increasing the  $\tilde{\chi}_1^0$  mass slightly decreases the annihilation cross section, which basically scales like  $1/m_{\tilde{\chi}_1^0}^2$  in this region.

In principle one can choose a renormalization scheme where the LSP mass is used as input in the on-shell renormalization of the  $\tilde{\chi}$  sector. However, such a scheme would lead to quite large corrections in some regions of parameter space [34]. Moreover, co-annihilation reactions play a significant role in determining the relic density of a higgsino-like LSP. If the LSP mass is kept fixed, there will be significant loop corrections to the masses of the other higgsino-like states,  $m_{\tilde{\chi}_2^0}$  and  $m_{\tilde{\chi}_1^\pm}$ ;‡ as a result, there would be large corrections to co-annihilation cross sections proceeding through exchange of a heavy (neutral or charged) Higgs boson. The total size of the correction to the relic density

---

\*In principle  $W^+W^-$  and  $ZZ$  final states can be produced via the  $s$ -channel exchange of the CP-even Higgs bosons, whose couplings to two neutralinos or two charginos do receive some corrections. However, these contributions are suppressed by the small size of the gaugino components of the (co-)annihilating states; moreover, since  $m_A^2 \gg M_Z^2$ , the couplings of the heavy CP-even Higgs boson  $H$  to two gauge bosons is very small. In practice our corrections to  $\tilde{\chi}_1^0$  couplings therefore do not significantly modify the (co-)annihilation cross sections into two gauge bosons.

†The corrections to the “top Yukawa” coupling of  $\tilde{\chi}_1^0$ , which is  $\propto \Delta N_{14}$ , does play a role in the tiny kink visible at the  $t\bar{t}$  threshold,  $\mu \simeq 180$  GeV.

‡A renormalization scheme where the masses of all three higgsino-like states were used as inputs would be very badly behaved indeed, since then no input mass would have significant dependence on  $M_1$  or  $M_2$ , leading to very large counterterms for these parameters [34].

near the heavy Higgs poles would then still be of similar size as in our scheme.

In the vicinity of the Higgs poles, our corrections to the wino- and bino-couplings of  $\tilde{\chi}_1^0$  (and, in co-annihilation reactions, of  $\tilde{\chi}_2^0$ , as well as the wino couplings of  $\tilde{\chi}_1^\pm$ ) do play a role. Note that the wino- and bino-components of  $\tilde{\chi}_1^0$  have opposite sign in this region of parameter space, which means that they add constructively to the  $\tilde{\chi}_1^0\tilde{\chi}_1^0(H, A)$  couplings. We see in Fig. 5a that in the region of the heavy Higgs poles, the relative corrections to  $N_{11}$  and  $N_{12}$  are both positive, leading to an increase of the magnitudes of the  $\tilde{\chi}_1^0\tilde{\chi}_1^0(H, A)$  couplings. For larger  $\mu$  the correction to  $N_{12}$  turns negative, helping to reduce the overall size of the corrections to the relic density in that region of parameter space.

The corrections to (the gaugino part of) Higgs couplings to  $\tilde{\chi}$  currents also play a role in the (co-)annihilation cross sections into one massive gauge boson and one heavy Higgs boson, which open around  $\mu = 310$  GeV, as well into the light Higgs boson  $h$  and one of the heavy Higgs bosons  $A, H, H^\pm$ , which become accessible for  $\mu > 322$  GeV; the former mostly proceed via the exchange of a heavy Higgs boson in the  $s$ -channel, while the latter also receive significant contributions from the exchange a gaugino-like  $\tilde{\chi}$  states in the  $t$ - or  $u$ -channel. With the exception of the region with strongest bino-higgsino mixing,  $\mu \simeq 400$  GeV, where the corrections to  $N_{12}$  are relatively large and negative, all relevant Higgs couplings are enhanced by our correction, thereby increasing the corresponding cross sections, whereas the increase of the mass still tends to reduce the cross section due to the proximity of the  $H, A$  poles. These two effects tend to cancel, reducing the overall size of the correction to the relic density to  $\leq 1.5\%$  for  $300 \text{ GeV} \leq \mu \leq 400 \text{ GeV}$ .

For yet larger  $\mu$ ,  $\tilde{\chi}_1^0$  becomes bino-like, as noted above. The absolute size of the correction to  $\Omega_{\tilde{\chi}_1^0}$  then increases with increasing  $\mu$ , as co-annihilation reactions, which are little affected by our corrections, become less important. Since the corrections increase the bino coupling of  $\tilde{\chi}_1^0$ , they reduce the relic density. The correction is somewhat smaller than in most of Fig. 3d since even at  $\mu = 600$  GeV final states containing one massive gauge boson and one Higgs boson, as well as diagrams with Higgs exchange in the  $s$ -channel, play significant roles; in both cases only one vertex gets corrected. Note finally that the correction is perfectly well-behaved at  $\mu = M_2 = 600$  GeV, as advertised (and in contrast to the scheme used in [32]).

Within standard cosmology, the  $\tilde{\chi}_1^0$  relic density reaches its desired value at  $\mu \simeq 460$  GeV, in the region of strong higgsino-bino mixing, where corrections to  $\Omega_{\tilde{\chi}_1^0}$  are negative. For smaller values of  $\mu$ ,  $\tilde{\chi}_1^0$  would only contribute a fraction of the total Dark Matter density.

#### 4.4 Co-annihilation with $\tilde{\tau}_1$

If the mass difference between the LSP and the next-lightest superparticle (NLSP) is sufficiently small, co-annihilation processes play a role in the determination of the LSP relic density [53]. This is generic for wino- as well as higgsino-like LSP, where  $\tilde{\chi}_1^\pm$  is automatically close in mass to  $\tilde{\chi}_1^0$ ; in case of higgsino-like LSP,  $\tilde{\chi}_2^0$  is also nearby. In this subsection we study co-annihilation of a bino-like LSP with the lightest stau state  $\tilde{\tau}_1$ . This is well motivated even within the framework of the minimal supergravity (mSUGRA) model [54]. The effect of co-annihilation can be described quite well [53] by introducing

an effective annihilation cross section, which is essentially the sum of the usual LSP (self-)annihilation cross section and the  $\tilde{\chi}_1^0 \tilde{\tau}_1$  and  $\tilde{\tau}_1 \tilde{\tau}_1$  annihilation cross sections, where the latter are suppressed by one and two powers, respectively, of the Boltzmann factor  $\exp[-T_F/(m_{\tilde{\tau}_1} - m_{\tilde{\chi}_1^0})]$ . Since the freeze-out temperature  $T_F$  is basically proportional to  $m_{\tilde{\chi}_1^0}$ , the Boltzmann suppression factor depends on the *relative* mass splitting between the LSP and the lighter stau.

We have assumed  $\mu = 600$  GeV and  $M_2 = 400$  GeV. All other input parameters are as described in (8), except that we have used  $m_A = 1.0$  TeV\*,  $m_{\tilde{\tau}_R} = M_1 + 5$  GeV and  $\tan\beta = 5$ . Note that the physical  $\tilde{\tau}_1$  mass is increased by the “ $D$ -term” contribution  $-\sin^2\theta_W \cos(2\beta)M_Z^2 > 0$ , and reduced by  $\tilde{\tau}_L - \tilde{\tau}_R$  mixing. For the given choice of parameters, we find a  $\tilde{\tau}_1 - \tilde{\chi}_1^0$  mass splitting of about 14 GeV, almost independent of  $M_1$  in the range shown in Fig. 6.

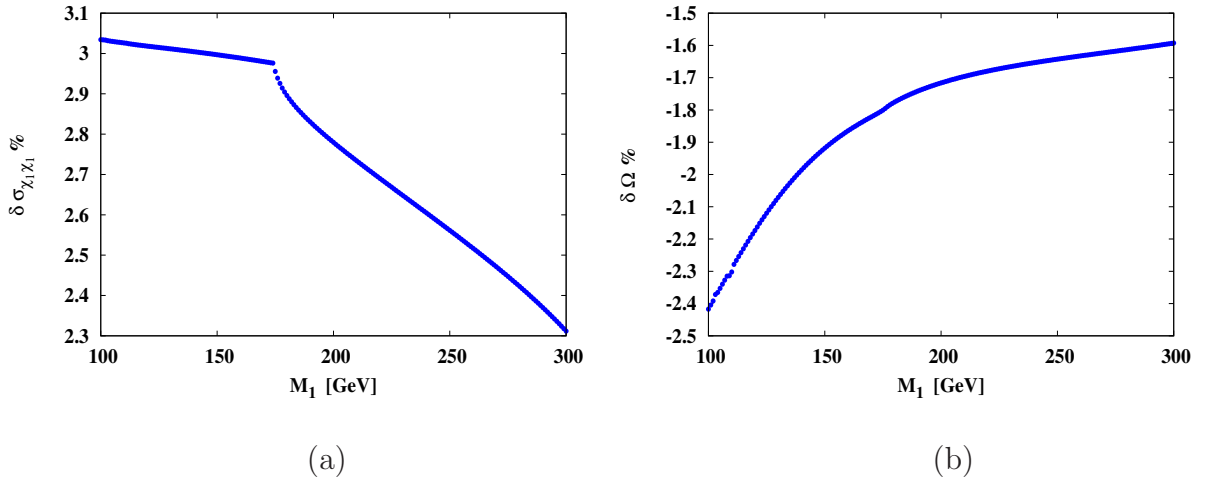


Figure 6: (a) Correction to the  $\tilde{\chi}_1^0$  annihilation cross section and (b) radiative correction to the relic density of  $\tilde{\chi}_1^0$  (in %) against  $M_1$ . Results are for  $M_2 = 0.4$  TeV,  $\mu = 0.6$  TeV,  $m_A = 1.0$  TeV,  $\tan\beta = 5$  and  $m_{\tilde{\tau}_R} = M_1 + 5$  GeV; the remaining parameters are as in our benchmark scenario (8).

In Fig. 6 (a), the correction to the  $\tilde{\chi}_1^0$  annihilation cross section is shown. Since  $\tilde{\tau}_1$  is much lighter than all other sfermions in the scenario considered here,  $\tilde{\chi}_1^0$  pairs dominantly annihilate into  $\tau^+ \tau^-$  pairs via  $\tilde{\tau}_1$  exchange in the  $t$ - or  $u$ -channel. Both vertices in these diagrams receive significant positive corrections, leading to an enhanced  $\tilde{\chi}_1^0$  annihilation cross section.

---

\*We have increased  $m_A$  in order to avoid the heavy Higgs poles, where `micrOMEGAs` (version 2.2.CPC.i) produces a spurious divergence in the co-annihilation cross section. This occurs because  $\tilde{\tau}_1 \rightarrow \tau + \tilde{\chi}_1^0$  can occur on-shell. As a result,  $\tilde{\tau}_1 + \tilde{\chi}_1^0 \rightarrow \tau + (A, H)$  can proceed through “exchange” of an on-shell  $\tilde{\chi}_1^0$ , giving an infinity in the (differential) cross section; note that  $\tilde{\chi}_1^0$  is stable, and hence has vanishing width. This divergence is not physical. In the present context, the very fast reactions  $\tilde{\tau}_1 \leftrightarrow \tilde{\chi}_1^0 + \tau$  help to maintain the relative equilibrium between the  $\tilde{\chi}_1^0$  and  $\tilde{\tau}_1$  densities at temperatures well below  $T_F$ . In the formalism of ref.[53] these fast reactions are integrated out to arrive at the effective Boltzmann equation for the  $\tilde{\chi}_1^0$  density. The removal of this unphysical divergence is a separate issue not related to the radiative corrections we are interested in, so we simply avoid it by increasing the masses of the heavy Higgs bosons.

At  $M_1 \sim 175$  GeV the relative size of the correction begins to diminish somewhat. At this point annihilation to a  $t\bar{t}$  pair opens. Increasing  $M_1$  along with  $m_{\tilde{\tau}_R}$  reduces the annihilation cross section into  $\tau^+\tau^-$  pairs roughly like the inverse square of the  $\tilde{\chi}_1^0$  mass, but increases several other cross sections. In particular, since  $\mu$  is kept fixed, increasing  $M_1$  increases higgsino–gaugino mixing, which leads to enhanced cross sections for  $W^+W^-$ ,  $ZZ$  as well as  $Zh$  final states. In some of these channels, as well as for the  $t\bar{t}$  channel, there is destructive interference between  $s$ –channel Higgs exchange and  $t$ – and  $u$ –channel diagrams. The corrections to the annihilation cross sections into  $W^+W^-$  and  $t\bar{t}$  final states are therefore negative (about  $-0.5\%$  and  $-3\%$ , respectively). This leads to a reduction of the relative size of the correction to the total  $\tilde{\chi}_1^0$  annihilation cross section.

The right frame of Fig. 6 shows that the correction to the  $\tilde{\chi}_1^0$  relic density is significantly smaller in magnitude than that to the  $\tilde{\chi}_1^0$  annihilation cross section. This is mostly due to co–annihilation contributions. Recall that the importance of these contributions depends on the *relative*  $\tilde{\tau}_1 - \tilde{\chi}_1^0$  mass splitting; since the absolute mass splitting remains approximately constant over the entire range of  $M_1$  shown, the relative mass splitting decreases approximately  $\propto 1/M_1$ . As a result, co–annihilation becomes more important at larger  $M_1$ .

The most important co–annihilation reactions are  $\tilde{\chi}_1^0\tilde{\tau}_1^\pm \rightarrow \tau^\pm + (\gamma, Z)$ , where only one vertex is corrected, as well as  $\tilde{\tau}_1^+\tilde{\tau}_1^- \rightarrow \gamma\gamma, \gamma Z$ , which proceed solely through (true) gauge interactions, which we do not correct. However,  $\tilde{\tau}_1^\pm\tilde{\tau}_1^\pm \rightarrow \tau^\pm\tau^\pm$  also contributes significantly, where again both vertices of the dominant  $\tilde{\chi}^0$  exchange diagrams get corrected. Nevertheless, our corrections affect the co–annihilation cross sections much less than the  $\tilde{\chi}_1^0$  annihilation cross section. Together with the increased importance of these co–annihilation contributions this explains the decline of the relative size of the corrections with increasing  $M_1$ . In the case at hand, co–annihilation is dominant for  $M_1 \geq 150$  GeV. For much larger values of  $M_1$ , the Boltzmann suppression factors are close to unity, and the relative size of the corrections stays approximately constant until one approaches the heavy Higgs poles (not shown).

Within standard cosmology, in the parameter space shown in Fig. 6, the  $\tilde{\chi}_1^0$  relic density is three to four times higher than the desired value. This could be corrected by also reducing the masses of some other sleptons, and/or further reducing  $m_{\tilde{\tau}_1}$ . In both cases the importance of co–annihilation contributions would increase, so that the relative corrections to the relic density would be similar to that in the high– $M_1$  region of Fig. 6.

## 5 Conclusions

In this paper we have studied the impact of the effective couplings, as introduced in [32], and of corrections to the neutralino and chargino masses, in the scheme introduced in ref.[34], on the calculation of the cosmological relic density of the lightest neutralino in the MSSM.

In Sec. 2 we analyzed the nature of the corrections captured by these effective couplings. We pointed out that they not only describe the difference in the running of true gauge couplings and gaugino couplings, but also corrections to the entries of the chargino and neutralino mass matrices that mix higgsino and gaugino states. Technically, these effective couplings include  $\tilde{\chi}$  two–point function corrections plus associated counterterms.

These corrections are thus enhanced by multiplicity factors, since all (s)fermions contribute similarly to the gaugino two-point functions. It has also been known for some time that the magnitude of these corrections increases logarithmically with the mass of heavy sfermions [28]. There is thus some reason to believe that they capture a large fraction of all electroweak radiative corrections; in case of  $\tilde{\chi}_2^0 \rightarrow f\bar{f}\tilde{\chi}_1^0$  decays this has been shown to be the case [33].

In Sec. 3 we briefly described how we incorporated these corrections into the **micrOMEGAs** program package [36]. The corrections apply to both the “gauge” and the “Yukawa” components of  $\tilde{\chi}\tilde{f}f$  couplings, as well as to the “gaugino” components of Higgs couplings to  $\tilde{\chi}$  currents. It should be noted that we use on-shell renormalization in the electroweak sector, whereas **micrOMEGAs** uses  $\overline{\text{MS}}$  inputs for the QED coupling and the weak mixing angle. We nevertheless compare with **micrOMEGAs** tree-level predictions when illustrating the effect of the corrections, see eq.(7).\*

Numerical results are shown in Sec. 4. We found that the corrections to  $\sigma(\tilde{\chi}_1^0\tilde{\chi}_1^0 \rightarrow e^+e^-)$  can reach +15% for wino-like  $\tilde{\chi}_1^0$ . However, in this case  $\tilde{\chi}_1^0$  dominantly annihilates into  $W^+W^-$  final states, which are relatively little affected by our corrections (only via  $s$ -channel Higgs exchange diagrams). The corrections to the *total*  $\tilde{\chi}_1^0$  annihilation cross section due to the effective couplings therefore never exceed 4% for our choice of squark masses near 1.5 TeV, i.e. not far beyond the current LHC lower bound. The correction to the  $\tilde{\chi}_1^0$  mass, which never exceed a couple of percent in our scheme, can lead to significantly larger corrections to the total annihilation cross section in the vicinity of Higgs poles. These mass corrections were shown to be especially important for higgsino-like LSP. In all cases the relative corrections to the relic density are slightly smaller than those to the (effective) annihilation cross section, since an increase of the latter also reduces the temperature at which  $\tilde{\chi}_1^0$  decouples from the thermal plasma.

It should be noted that the corrections to the relic density are frequently comparable to, or larger than, the present observational uncertainty on the total Dark Matter density (in the framework of standard cosmology); this uncertainty is expected to be reduced significantly as soon as the PLANCK collaboration completes the analysis of their data on the cosmic microwave anisotropies.

Note also that the effective couplings as defined in [32] include certain diagrams contributing to a complete one-loop calculation of  $\sigma(\tilde{\chi}_1^0\tilde{\chi}_1^0 \rightarrow f\bar{f})$  *exactly*, namely the two-point function corrections on the external  $\tilde{\chi}_1^0$  lines with fermion-sfermion loops. Their inclusion into an “effective tree-level” calculation, as done here, can therefore be understood as a first step towards a full electroweak one-loop calculation [16], which is however computationally far more complex. We use the same effective couplings also when a  $\tilde{\chi}$  is exchanged in the  $t$ - or  $u$ -channel, which contributes to sfermion co-annihilation; since here  $\tilde{\chi}$  is off-shell, the effective couplings include two-point function corrections to its propagator only approximately, but the relation with the exact calculation is still fairly straightforward.

The situation is a bit more complicated for the Higgs couplings to  $\tilde{\chi}$  currents. Here

---

\*The corrected couplings  $g(N + \Delta N)$ ,  $g(U + \delta U)$ ,  $g(V + \Delta V)$  are scheme-independent up to two-loop terms; however, the tree-level couplings  $gN$  etc. are scheme-dependent already at one-loop order. We use **micrOMEGAs** choices here since this is currently the industry standard for LSP relic density calculations.



we correct only the gaugino part of the coupling. In the limit of vanishing gaugino–higgsino mixing, this corresponds to including only the gaugino to gaugino and higgsino to gaugino two–point functions, but no higgsino to higgsino or gaugino to higgsino diagrams. However, in realistic situations with non–vanishing  $\tilde{\chi}$  mixing this no longer corresponds to a complete subclass of diagrams. Moreover, it has been shown some time ago [55] that at least some corrections to  $Z\tilde{\chi}_1^0\tilde{\chi}_1^0$  couplings can be described in terms of neutralino two–point function corrections. There might thus be further scope for extension of the effective coupling scheme to Higgs couplings, and/or to couplings to  $W$  and  $Z$  bosons to  $\tilde{\chi}$  states. We plan to investigate these issues in future.

## Acknowledgment

We thank K. Williams and D. Lopez–Val for numerous discussions. We also thank F. Boudjema for discussions on `micrOMEGAs` and issues of gauge invariance. AC and SK acknowledge support from the Bonn Cologne Graduate School of Physics and Astronomy. This work was partially supported by the DFG Transregio TR33 “The Dark Side of the Universe”, and partly by the German Bundesministerium für Bildung und Forschung (BMBF) under Contract No. 05HT6PDA. S.K. acknowledges partial support from the European Union FP7 ITN INVISIBLES (Marie Curie Actions, PITN- GA-2011- 289442).

## A Weak Sector

We apply on–shell renormalization of the electroweak sector, where  $M_W$  and  $M_Z$  are physical (pole) masses, and  $\cos\theta_W = M_W/M_Z$ . This gives [56]:

$$\begin{aligned}\delta M_W^2 &= \widetilde{\Re}\Sigma_{WW}(M_W^2); \\ \delta M_Z^2 &= \widetilde{\Re}\Sigma_{ZZ}(M_Z^2); \\ \delta \cos\theta_W &= \frac{M_W}{M_Z} \left( \frac{\delta M_W}{M_W} - \frac{\delta M_Z}{M_Z} \right).\end{aligned}\tag{9}$$

Here  $\Sigma_{WW}$  and  $\Sigma_{ZZ}$  are the transverse components of the diagonal  $W$  and  $Z$  two–point functions in momentum space, respectively; only the real parts of the loop functions should be included as indicated by the  $\widetilde{\Re}$  symbols. Note that, while the definitions of these three counterterms are formally as in the SM, in the MSSM there are many new contributions to  $\Sigma_{WW}$  and  $\Sigma_{ZZ}$  involving loops of superparticles and additional Higgs bosons.

In our treatment we have to calculate the counterterms for  $M_W$ ,  $M_Z$  and  $\cos\theta_W$  twice: for the purpose of computing effective couplings, we only include loops of matter fermions and sfermions, but for the correction to neutralino and chargino masses [34] we include the full MSSM contributions.

The  $SU(2)$  gauge coupling is given by  $g = e/\sin\theta_W$ , where the  $e$  is the QED couplings constants, the renormalization of which is discussed in the following Appendix. The counterterm  $\delta g$  is then given by

$$\delta g = \frac{\delta e}{\sin\theta_W} - g \frac{\delta \sin\theta_W}{\sin\theta_W} = \frac{\delta e}{\sin\theta_W} + g \frac{\cos\theta_W}{\sin^2\theta_W} \delta \cos\theta_W,\tag{10}$$

where  $\delta \cos \theta_W$  has been given in eq.(9), and  $\delta e = e(M_Z)\delta Z_e^{e(M_Z^2)}$  with  $\delta Z_e^{e(M_Z^2)}$  given in eq.(20) below. The counterterm  $\delta g$  is needed only in the calculation of effective couplings, so only matter (s)fermion loops are included.

Similarly, the counterterm  $\delta \tan \theta_W$  needed in eqs.(4) is to one-loop order given by

$$\delta \tan \theta_W = -\frac{\delta \cos \theta_W}{\sin \theta_W \cos^2 \theta_W}. \quad (11)$$

## B Charge Renormalization

The on-shell renormalization condition for the electric charge requires the electric charge to be equal to the full  $ee\gamma$  coupling for on-shell external particles in the Thomson limit. This leads to

$$e^{\text{bare}} \rightarrow e(0) (1 + \delta Z_e^{(0)}). \quad (12)$$

The renormalization constant is adjusted to cancel the loop corrections to the  $ee\gamma$  vertex in this limit. This gives [57]:

$$\delta Z_e^{(0)} = \frac{1}{2} \frac{\partial}{\partial q^2} \Sigma_{\gamma\gamma}(q^2)|_{q^2=0} + \tan \theta_W \frac{\Sigma_{\gamma Z}(0)}{M_Z^2}, \quad (13)$$

where the  $\Sigma$  again refer to the transverse part of the corresponding two-point functions. We can thus identify the renormalized charge  $e(0) = \sqrt{4\pi\alpha(0)}$  where  $\alpha(0) = 1/137.036\dots$  is the fine structure constant, as defined in the Thomson limit.

While pure on-shell renormalization of  $e$  is perfectly fine in a theory of photons and electrons, a problem arises in the presence of light quarks. The counterterm  $\delta Z_e^{(0)}$  receives contributions from loops involving a light fermion  $f$  that scale  $\propto \log(m_f^2)$ , leading to terms proportional to  $\alpha \log(m_f^2/s)$  in corrections to physical processes at some energy scale  $s$ ; these can be understood as describing the running of the QED coupling. The problem is that the masses of the light  $u, d, s$  (and, to some extent,  $c$ ) quarks aren't well known, and in fact are difficult to define in the Thomson limit.

Fortunately this dependence on the light quark masses can be traded for a dependence on experimentally measured cross sections for  $e^+e^-$  annihilation into hadronic final states. To that end, one writes

$$\frac{\partial}{\partial q^2} \Sigma_{\gamma\gamma}^{\text{light } f \text{ in loops}}(q^2)|_{q^2=0} = \Delta\alpha + \frac{1}{M_Z^2} \widetilde{\Re} \Sigma_{\gamma\gamma}^{\text{light } f \text{ in loops}}(M_Z^2), \quad (14)$$

where  $\Delta\alpha$  is a finite quantity; moreover, the second term in eq.(14) is finite for  $m_f \rightarrow 0$ , so that the  $u, d, s$  masses can be neglected when evaluating this term.  $\Delta\alpha$  can be split into two parts: the contribution from the  $e, \mu, \tau$  leptons and the contribution from the light quarks (i.e. all except  $t$ ),  $\Delta\alpha = \Delta\alpha_{\text{lep}} + \Delta\alpha_{\text{had}}$ .  $\Delta\alpha_{\text{lep}}$  has been calculated up to 3-loop order as [58]

$$\Delta\alpha_{\text{lep}} = 0.031497687, \quad (15)$$

while  $\Delta\alpha_{\text{had}}$  can be extracted from experiment via a dispersion relation [59]:

$$\Delta\alpha_{\text{had}} = 0.027626 \pm 0.00138. \quad (16)$$

This leads us to

$$\delta Z_e^{(0)} = \frac{1}{2} \frac{\partial}{\partial q^2} [\Sigma_{\gamma\gamma}^{\text{all loops}}(q^2)|_{q^2=0} - \Sigma_{\gamma\gamma}^{\text{light } f \text{ in loops}}(q^2)|_{q^2=0}] \quad (17)$$

$$+ \frac{1}{2} \Delta\alpha + \frac{1}{2M_Z^2} \widetilde{\Re} \Sigma_{\gamma\gamma}^{\text{light } f \text{ in loops}}(M_Z^2) + \tan \theta_W \frac{\Sigma_{\gamma Z}(0)}{M_Z^2}. \quad (18)$$

One can achieve even higher accuracy by re-summing the light fermion correction. This corresponds to using the “running on-shell” coupling  $\alpha(M_Z^2) = \alpha(0)/(1 - \Delta\alpha) = 1/128.93$  as input (“tree-level”) coupling.<sup>†</sup> The corresponding renormalization constant becomes:

$$\begin{aligned} e^{\text{bare}} \rightarrow e(0) (1 + \delta Z_e^{(0)}) &= e(0) \left( 1 + \frac{1}{2} \Delta\alpha - \frac{1}{2} \Delta\alpha \right) (1 + \delta Z_e^{(0)}) \\ &= e(M_Z^2) \left( 1 + \delta Z_e^{e(M_Z^2)} + \text{higher order} \right). \end{aligned} \quad (19)$$

Thus,

$$\begin{aligned} \delta Z_e^{e(M_Z^2)} &= \delta Z_e^{(0)} - \frac{\Delta\alpha}{2} \\ &= \frac{1}{2} \frac{\partial}{\partial q^2} \Sigma_{\gamma\gamma}^{\text{all loops}}(q^2)|_{q^2=0} - \frac{1}{2} \frac{\partial}{\partial q^2} \Sigma_{\gamma\gamma}^{\text{light } f \text{ in loops}}(q^2)|_{q^2=0} \\ &+ \frac{1}{2M_Z^2} \widetilde{\Re} \Sigma_{\gamma\gamma}^{\text{light } f \text{ in loops}}(M_Z^2) + \tan \theta_W \frac{\Sigma_{\gamma Z}(0)}{M_Z^2}. \end{aligned} \quad (20)$$

We need  $\delta Z_e^{e(M_Z^2)}$  only in the calculation of effective couplings, hence only the matter (s)fermion loop contributions are included here.

## C Higgs Sector

The only relevant counterterm determined from this sector is  $\delta \tan \beta$ . It is fixed by forbidding transitions between the CP-odd Higgs boson  $A$  and the  $Z$  boson on the  $A$  mass shell [60, 61, 62]. This gives:

$$\delta \tan \beta = \frac{1}{2M_Z \cos^2 \beta} \Im(\Sigma_{AZ}(m_A^2)). \quad (21)$$

Note that the couplings of  $A$  contain an extra factor of imaginary  $i$  relative to the gauge couplings. Therefore the imaginary part of the two-point function appears in eq.(21); this contains the real (dispersive), infinite, part of the loop function.

The counterterms for  $\cos \beta$  and  $\sin \beta$  are thus:

$$\delta \cos \beta = -\cos^3 \beta \tan \beta \delta \tan \beta, \quad (22)$$

---

<sup>†</sup>As mentioned in Sec. 3, this differs slightly from the running  $\overline{\text{MS}}$  coupling  $\hat{\alpha}(M_Z) = 1/127.944$  often used in tree-level calculations of electroweak processes; see e.g. the review by Erler and Langacker in [46].

$$\delta \sin \beta = \cos^3 \beta \delta \tan \beta. \quad (23)$$

The fermion loop contribution to  $\Sigma_{AZ}$  is proportional to the mass of the fermion in the loop. In case of SM quarks and leptons, this gives an additional factor of the corresponding Yukawa coupling times  $M_W/g$ . These contributions to  $\delta \tan \beta$  should therefore be counted as  $\mathcal{O}(\lambda^2)$ , not as  $\mathcal{O}(\lambda g)$ , the second factor of  $\lambda$  stemming from the coupling of  $A$  to the SM fermion in the loop.

These counterterms are needed both for the calculation of one-loop corrected neutralino and chargino masses and for the evaluation of the effective couplings. As in case of the counterterms to the  $W$  and  $Z$  masses, in the former case all MSSM loop contributions are included, while in the latter case only matter (s)fermion loops are included.

## D Chargino and Neutralino Sector

In this appendix, we describe the determination of the relevant counterterms in the chargino–neutralino sector of the MSSM, closely following the discussion in [32, 35, 63, 34].

The one-loop mass eigenstates can be related to the tree level mass eigenstates through wave function renormalization:

$$\tilde{\chi}_i^{\text{bare}} = (\delta_{ij} + \frac{1}{2}\delta Z_{ij}^L P_L + \frac{1}{2}\delta Z_{ij}^R P_R) \tilde{\chi}_j^{\text{renormalized}}. \quad (24)$$

where  $P_L$  and  $P_R$  are the chiral projectors. This relation holds for both the chargino sector, with  $\tilde{\chi}_i \equiv \tilde{\chi}_i^+$ ,  $i \in \{1, 2\}$ , and the neutralino sector, with  $\tilde{\chi}_i \equiv \tilde{\chi}_i^0$ ,  $i \in \{1, 2, 3, 4\}$ . The entries of the mixing matrices  $N$ ,  $U$  and  $V$  have been chosen to be identical to their tree level values [63].

The corresponding masses receive explicit corrections from one-loop diagrams, which can be written as

$$\delta m_f = \frac{1}{2}m_f \left[ \widetilde{\Re} \Sigma_{ff}^{VL}(m_f^2) + \widetilde{\Re} \Sigma_{ff}^{VR}(m_f^2) \right] + \frac{1}{2} \left[ \widetilde{\Re} \Sigma_{ff}^{SL}(m_f^2) + \widetilde{\Re} \Sigma_{ff}^{SR}(m_f^2) \right], \quad (25)$$

where  $f$  denotes a fermion species with mass  $m_f$ .  $\widetilde{\Re}$  again denotes the real parts of the loop integrals involved and the  $\Sigma$  refer to various terms in the general two-point function connecting fermions  $f$  and  $f'$  in momentum space:

$$\Sigma_{ff'}(p) = \not{p} [P_L \Sigma_{ff'}^{VL}(p) + P_R \Sigma_{ff'}^{VR}(p)] + P_L \Sigma_{ff'}^{SL}(p) + P_R \Sigma_{ff'}^{SR}(p). \quad (26)$$

Only the case  $f = f'$  is needed in eq.(25), but we will need off-diagonal two-point functions for the determination of the wave function counterterms.

The corrections of eq.(25) are in general divergent. These divergencies are absorbed into counterterms to the mass matrices  $M^c$  and  $M^n$  of the charginos and the neutralinos respectively, i.e.

$$M^{\text{bare}} = M^{\text{renormalized}} + \delta M. \quad (27)$$

As usual, we define the physical (on-shell) masses as poles of the real parts of the (one-loop corrected) propagators. The physical chargino masses are then given by,

$$m_{\tilde{\chi}_i^+}^{\text{os}} = m_{\tilde{\chi}_i^+} + (U^* \delta M^c V^{-1})_{ii} - \delta m_{\tilde{\chi}_i^+}; \quad (28)$$

the corresponding expression for the neutralinos is

$$m_{\tilde{\chi}_i^0}^{\text{os}} = m_{\tilde{\chi}_i^0} + (N^* \delta M^n N^{-1})_{ii} - \delta m_{\tilde{\chi}_i^0}. \quad (29)$$

The masses  $m_{\tilde{\chi}_i^{+,0}}$  appearing on the right-hand sides of eqs.(28) and (29) are the (finite) tree-level masses.  $\delta m_{\tilde{\chi}_i^{+,0}}$  are the explicit loop corrections of eq.(25) as applied to the charginos and neutralinos. Finally,  $\delta M^{c,n}$  are the counterterm matrices of eq.(27) for the chargino and neutralino sector, which we yet have to determine.

To one-loop order counterterms to products like  $M_W \sin \beta$  can be written as  $(\delta M_W) \sin \beta + M_W \delta \sin \beta$ , and so on.

Altogether, the tree-level chargino and neutralino mass matrices depend on seven parameters, hence there are seven different counterterms:  $\delta M_W$ ,  $\delta M_Z$ ,  $\delta \theta_W$ ,  $\delta \tan \beta$ ,  $\delta M_1$ ,  $\delta M_2$  and  $\delta \mu$ . The first three of these already appear in the SM, see Appendix A.  $\delta \tan \beta$  has been fixed in the Higgs sector, see Appendix C.

Hence only the counterterms to  $M_1$ ,  $M_2$  and  $\mu$  remain to be fixed in the chargino and neutralino sector. This means that we can only chose three of the six masses in this sector to be input masses which are not changed by loop corrections, i.e. only three of the six “tree-level” masses are physical (all-order) masses. We choose the wino-like chargino mass, the bino-like and higgsino-like neutralino masses as inputs (i.e. physical masses). Ref.[34] explains in detail why this particular choice of input states leads to the most stable perturbative expansion, by avoiding spurious large corrections. The other three masses will receive finite, but non-zero corrections. The remaining counterterms can then be computed from eqs.(28) and (29):

$$\delta M_1 = -\frac{N_{M_1}}{D}, \quad (30)$$

$$\delta M_2 = \frac{N_{M_2}}{D}, \quad (31)$$

$$\delta \mu = \frac{N_\mu}{D}, \quad (32)$$

where

$$D = 2N_{i3}^* N_{i4}^* N_{j1}^{*2} U_{k1}^* V_{k1}^* - 2N_{i1}^{*2} N_{j3}^* N_{j4}^* U_{k1}^* V_{k1}^* + N_{i2}^{*2} N_{j1}^{*2} U_{k2}^* V_{k2}^* - N_{i1}^{*2} N_{j2}^{*2} U_{k2}^* V_{k2}^*, \quad (33)$$

$$\begin{aligned} N_\mu = & - \left[ N_{j1}^{*2} \left( \delta m_{\tilde{\chi}_i^0} - 2\delta M_{13}^n N_{i1}^* N_{i3}^* - 2\delta M_{23}^n N_{i2}^* N_{i3}^* - 2\delta M_{14}^n N_{i1}^* N_{i4}^* - 2\delta M_{24}^n N_{i2}^* N_{i4}^* \right) \right. \\ & + N_{i1}^{*2} \left( -\delta m_{\tilde{\chi}_j^0} + 2\delta M_{13}^n N_{j1}^* N_{j3}^* + 2\delta M_{23}^n N_{j2}^* N_{j3}^* + 2\delta M_{14}^n N_{j1}^* N_{j4}^* + 2\delta M_{24}^n N_{j2}^* N_{j4}^* \right) \left. \right] U_{k1}^* V_{k1}^* \\ & + \left( -N_{i2}^{*2} N_{j1}^{*2} + N_{i1}^{*2} N_{j2}^{*2} \right) \left( -\delta m_{\tilde{\chi}_k^+} + \delta M_{21}^c U_{k2}^* V_{k1}^* + \delta M_{12}^c U_{k1}^* V_{k2}^* \right), \end{aligned} \quad (34)$$

$$\begin{aligned} N_{M_2} = & 2\delta m_{\tilde{\chi}_k^+} N_{i3}^* N_{i4}^* N_{j1}^{*2} - 2\delta m_{\tilde{\chi}_k^+} N_{i1}^{*2} N_{j3}^* N_{j4}^* - 2\delta M_{21}^c N_{i3}^* N_{i4}^* N_{j1}^{*2} U_{k2}^* V_{k1}^* \\ & + 2\delta M_{21}^c N_{i1}^{*2} N_{j3}^* N_{j4}^* U_{k2}^* V_{k1}^* - 2\delta M_{12}^c N_{i3}^* N_{i4}^* N_{j1}^{*2} U_{k1}^* V_{k2}^* - \delta m_{\tilde{\chi}_j^0} N_{i1}^{*2} U_{k2}^* V_{k2}^* \\ & + \delta M_{12}^c N_{i1}^{*2} N_{j3}^* N_{j4}^* U_{k1}^* V_{k2}^* + \delta m_{\tilde{\chi}_i^0} N_{j1}^{*2} U_{k2}^* V_{k2}^* - 2\delta M_{13}^n N_{i1}^* N_{i3}^* N_{j1}^{*2} U_{k2}^* V_{k2}^* \\ & - 2\delta M_{23}^n N_{i2}^* N_{i3}^* N_{j1}^{*2} U_{k2}^* V_{k2}^* - 2\delta M_{14}^n N_{i1}^* N_{i4}^* N_{j1}^{*2} U_{k2}^* V_{k2}^* - 2\delta M_{24}^n N_{i2}^* N_{i4}^* N_{j1}^{*2} U_{k2}^* V_{k2}^* \\ & + 2\delta M_{13}^n N_{i1}^{*2} N_{j3}^* N_{j4}^* U_{k2}^* V_{k2}^* + 2\delta M_{23}^n N_{i1}^{*2} N_{j2}^* N_{j3}^* U_{k2}^* V_{k2}^* + 2\delta M_{14}^n N_{i1}^{*2} N_{j1}^* N_{j4}^* U_{k2}^* V_{k2}^* \\ & + 2\delta M_{24}^n N_{i1}^{*2} N_{j2}^* N_{j4}^* U_{k2}^* V_{k2}^*, \end{aligned} \quad (35)$$

$$\begin{aligned}
N_{M_1} = & 2\delta m_{\tilde{\chi}_k^+} N_{i3}^* N_{i4}^* N_{j2}^{*2} - 2\delta m_{\tilde{\chi}_k^+} N_{i2}^{*2} N_{j3}^* N_{j4}^* - 2\delta m_{\tilde{\chi}_j^0} N_{i3}^* N_{i4}^* U_{k1}^* V_{k1}^* - \delta m_{\tilde{\chi}_j^0} N_{i2}^{*2} U_{k2}^* V_{k2}^* \\
& - 2\delta M_{14}^n N_{i1}^* N_{i4}^* N_{j2}^{*2} U_{k2}^* V_{k2}^* - 2\delta M_{24}^n N_{i2}^* N_{i4}^* N_{j2}^{*2} U_{k2}^* V_{k2}^* + 2\delta M_{13}^n N_{i2}^{*2} N_{j1}^* N_{j3}^* U_{k2}^* V_{k2}^* \\
& + 2\delta M_{23}^n N_{i2}^{*2} N_{j2}^* N_{j3}^* U_{k2}^* V_{k2}^* + 2\delta M_{14}^n N_{i2}^{*2} N_{j1}^* N_{j4}^* U_{k2}^* V_{k2}^* + 2\delta M_{24}^n N_{i2}^{*2} N_{j2}^* N_{j4}^* U_{k2}^* V_{k2}^* \\
& - 2\delta M_{12}^c N_{i3}^* N_{i4}^* N_{j2}^{*2} U_{k1}^* V_{k2}^* + 2\delta M_{12}^c N_{i2}^{*2} N_{j3}^* N_{j4}^* U_{k1}^* V_{k2}^* + 4\delta M_{13}^n N_{i3}^* N_{i4}^* N_{j1}^* N_{j3}^* U_{k1}^* V_{k1}^* \\
& + 4\delta M_{23}^n N_{i3}^* N_{i4}^* N_{j2}^* N_{j3}^* U_{k1}^* V_{k1}^* - 2\delta M_{13}^n N_{i1}^* N_{i3}^* N_{j2}^{*2} U_{k2}^* V_{k2}^* - 2\delta M_{23}^n N_{i2}^* N_{i3}^* N_{j2}^{*2} U_{k2}^* V_{k2}^* \\
& + 4\delta M_{14}^n N_{i3}^* N_{i4}^* N_{j1}^* N_{j4}^* U_{k1}^* V_{k1}^* + 4\delta M_{24}^n N_{i3}^* N_{i4}^* N_{j2}^* N_{j4}^* U_{k1}^* V_{k1}^* + 2\delta m_{\tilde{\chi}_i^0} N_{j3}^* N_{j4}^* U_{k1}^* V_{k1}^* \\
& - 4\delta M_{24}^n N_{i2}^* N_{i4}^* N_{j3}^* N_{j4}^* U_{k1}^* V_{k1}^* - 2\delta M_{21}^c N_{i3}^* N_{i4}^* N_{j2}^{*2} U_{k2}^* V_{k1}^* + 2\delta M_{21}^c N_{i2}^{*2} N_{j3}^* N_{j4}^* U_{k2}^* V_{k1}^* \\
& - 4\delta M_{13}^n N_{i1}^* N_{i3}^* N_{j3}^* N_{j4}^* U_{k1}^* V_{k1}^* - 4\delta M_{23}^n N_{i2}^* N_{i3}^* N_{j3}^* N_{j4}^* U_{k1}^* V_{k1}^* - 4\delta M_{14}^n N_{i1}^* N_{i4}^* N_{j3}^* N_{j4}^* U_{k1}^* V_{k1}^* \\
& + \delta m_{\tilde{\chi}_i^0} N_{j2}^{*2} U_{k2}^* V_{k2}^*. \tag{36}
\end{aligned}$$

Here  $i$  and  $j$  are the indices of the two neutralino input states, and  $k$  is the index of the chargino input state; the counterterms are symmetric under  $i \leftrightarrow j$ , both  $D$  and the numerators being antisymmetric. Since we take input states with fixed physical characteristics (bino-, wino- or higgsino-like), the numerical values of  $i, j, k$  will depend on (the ordering of) the parameters  $M_1, M_2$  and  $\mu$ ; see ref.[34] for further details.

These counterterms are needed both for the calculation of the one-loop corrected chargino and neutralino masses, where all MSSM loop contributions have been included in the evaluation of eq.(25), and for the calculation of effective couplings (see below), where only matter (s)fermion loop contributions have been included.

The diagonal wave-function counterterms are determined by normalizing the residues of the propagators [35, 32]:

$$\delta Z_i^{L,R} = -\widetilde{\Re}\Sigma_{ii}^{VL,VR}(m_{\tilde{\chi}_i}^2) - m_{\tilde{\chi}_i}^2 \left( \widetilde{\Re}\Sigma_{ii}^{VL'}(m_{\tilde{\chi}_i}^2) + \widetilde{\Re}\Sigma_{ii}^{VR'}(m_{\tilde{\chi}_i}^2) \right) - 2m_{\tilde{\chi}_i} \widetilde{\Re}\Sigma_{ii}^{SL,SR'}(m_{\tilde{\chi}_i}^2). \tag{37}$$

The prime denotes derivative with respect to the external momentum squared. This expression holds both for charginos [where these counterterms had an additional superscript + in eqs.(4)] and neutralinos.

The off-diagonal wave-function renormalization counterterms are determined by demanding that the corresponding off-diagonal two-point correlation functions vanish for on-shell external momenta [35, 32]. This gives:<sup>‡</sup>

$$\delta Z_{ij}^L = \frac{2 \left( m_{\tilde{\chi}_i} \hat{\Sigma}_{ij}^{SL}(m_{\tilde{\chi}_j}^2) + m_{\tilde{\chi}_j} \hat{\Sigma}_{ij}^{SR}(m_{\tilde{\chi}_j}^2) + m_{\tilde{\chi}_i} m_{\tilde{\chi}_j} \hat{\Sigma}_{ij}^{VR}(m_{\tilde{\chi}_j}^2) + m_{\tilde{\chi}_j}^2 \hat{\Sigma}_{ij}^{VL}(m_{\tilde{\chi}_j}^2) \right)}{m_{\tilde{\chi}_i}^2 - m_{\tilde{\chi}_j}^2}, \tag{38}$$

$$\delta Z_{ij}^R = \frac{2 \left( m_{\tilde{\chi}_i} \hat{\Sigma}_{ij}^{SR}(m_{\tilde{\chi}_j}^2) + m_{\tilde{\chi}_j} \hat{\Sigma}_{ij}^{SL}(m_{\tilde{\chi}_j}^2) + m_{\tilde{\chi}_i} m_{\tilde{\chi}_j} \hat{\Sigma}_{ij}^{VL}(m_{\tilde{\chi}_j}^2) + m_{\tilde{\chi}_j}^2 \hat{\Sigma}_{ij}^{VR}(m_{\tilde{\chi}_j}^2) \right)}{m_{\tilde{\chi}_i}^2 - m_{\tilde{\chi}_j}^2}, \tag{39}$$

where,

$$\hat{\Sigma}_{ij}^{VL,VR} = \widetilde{\Re}\Sigma_{ij}^{VL,VR}, \quad \hat{\Sigma}_{ij}^{SL} = \widetilde{\Re}\Sigma_{ij}^{SL} - \delta\tilde{m}_{ij}, \quad \hat{\Sigma}_{ij}^{SR} = \widetilde{\Re}\Sigma_{ij}^{SR} - \delta\tilde{m}_{ji}^*. \tag{40}$$

---

<sup>‡</sup>Note that our  $\Sigma_{ij}(m_{\tilde{\chi}}^2)$  corresponds to  $\Sigma^{ji}(m_{\tilde{\chi}}^2)$  of FormCalc.



These expressions again hold for both charginos and neutralinos, where the latter were labeled with an additional superscript + in eqs.(4) in the main text. Here  $\delta\tilde{m}_{ij}$  denotes  $(U^*\delta M^c V^{-1})_{ij}$  and  $(N^*\delta M^n N^{-1})_{ij}$  for charginos and neutralinos, respectively. The calculation of the counterterm matrices  $\delta M^c$  and  $\delta M^n$  has been discussed in the first part of this Appendix. Hermiticity implies the following relations:

$$\Sigma_{ij}^{SR}(q^2) = \Sigma_{ji}^{SL*}(q^2), \quad \Sigma_{ij}^{SL}(q^2) = \Sigma_{ji}^{SR*}(q^2), \quad \Sigma_{ij}^{VL}(q^2) = \Sigma_{ji}^{VL*}(q^2), \quad \Sigma_{ij}^{VR}(q^2) = \Sigma_{ji}^{VR*}(q^2).$$

Neutralinos are Majorana fermions. Consequently the following additional relations [35, 63] hold:

$$\Sigma_{ij}^{RS}(q^2) = \Sigma_{ji}^{RS}(q^2), \quad \Sigma_{ij}^{LS}(q^2) = \Sigma_{ji}^{LS}(q^2), \quad \Sigma_{ij}^{LV}(q^2) = \Sigma_{ji}^{RV}(q^2).$$

These relations can be used to further simplify eqs.(40) as applied to the neutralinos [35, 63].

Note finally that neutralino couplings may be purely imaginary even if CP is conserved; this is true for states corresponding to negative eigenvalues of the neutralino mass matrix. Since  $\Re$  *only* acts on the loop functions, these imaginary parts have to be kept in eqs.(37)–(39); in fact, they are necessary to yield finite results in eqs.(38), (39) for  $m_{\tilde{\chi}_i^0} = m_{\tilde{\chi}_j^0}$ , which is possible if  $M_1 M_2 < 0$ . In this case  $\tilde{\chi}_i^0$  and  $\tilde{\chi}_j^0$  can be combined into a Dirac neutralino state, and the corresponding “off-diagonal” wave function renormalization becomes part of the diagonal wave function renormalization of this Dirac neutralino. Degenerate charginos can only occur if  $\tan\beta = 1$ , which is excluded by Higgs mass bounds, or in the presence of nontrivial CP-violating phases in the chargino mass matrix.

## References

- [1] **WMAP** Collaboration, E. Komatsu *et al.*, “Seven-Year Wilkinson Microwave Anisotropy Probe (WMAP) Observations: Cosmological Interpretation,” *Astrophys. J. Suppl.* **192** (2011) 18, [arXiv:1001.4538 \[astro-ph.CO\]](#).
- [2] [http://www.rssd.esa.int/index.php?project=PLANCK&page=dev\\_news](http://www.rssd.esa.int/index.php?project=PLANCK&page=dev_news).
- [3] E. Kolb and M. Turner, *The Early Universe*. Westview Press, 1994.
- [4] G. F. Giudice, E. W. Kolb, and A. Riotto, “Largest temperature of the radiation era and its cosmological implications,” *Phys.Rev.* **D64** (2001) 023508, [arXiv:hep-ph/0005123 \[hep-ph\]](#).
- [5] N. Fornengo, A. Riotto, and S. Scopel, “Supersymmetric dark matter and the reheating temperature of the universe,” *Phys.Rev.* **D67** (2003) 023514, [arXiv:hep-ph/0208072 \[hep-ph\]](#).
- [6] M. Drees, H. Iminniyaz, and M. Kakizaki, “Constraints on the very early universe from thermal WIMP dark matter,” *Phys.Rev.* **D76** (2007) 103524, [arXiv:0704.1590 \[hep-ph\]](#).
- [7] M. Drees, R. Godbole, and P. Roy, *Theory and phenomenology of sparticles : An Account of four - dimensional N = 1 supersymmetry in high energy physics*. World Scientific, 2004.

- [8] T. Ibrahim and P. Nath, “The neutron and the lepton EDMs in MSSM, large CP violating phases, and the cancellation mechanism,” *Phys. Rev.* **D58** (1998) 111301, [arXiv:hep-ph/9807501](#).
- [9] M. Pospelov and A. Ritz, “Electric dipole moments as probes of new physics,” *Annals Phys.* **318** (2005) 119–169, [arXiv:hep-ph/0504231](#).
- [10] T. Falk, K. A. Olive, and M. Srednicki, “Heavy sneutrinos as dark matter,” *Phys.Lett.* **B339** (1994) 248–251, [arXiv:hep-ph/9409270](#) [[hep-ph](#)].
- [11] M. Drees, G. Jungman, M. Kamionkowski, and M. M. Nojiri, “Neutralino annihilation into gluons,” *Phys.Rev.* **D49** (1994) 636–647, [arXiv:hep-ph/9306325](#) [[hep-ph](#)].
- [12] B. Herrmann and M. Klasen, “SUSY-QCD Corrections to Dark Matter Annihilation in the Higgs Funnel,” *Phys. Rev.* **D76** (2007) 117704, [arXiv:0709.0043](#) [[hep-ph](#)].
- [13] A. Freitas, “Radiative corrections to co-annihilation processes,” *Phys.Lett.* **B652** (2007) 280–284, [arXiv:0705.4027](#) [[hep-ph](#)].
- [14] B. Herrmann, M. Klasen, and K. Kovarik, “Neutralino Annihilation into Massive Quarks with SUSY-QCD Corrections,” *Phys. Rev.* **D79** (2009) 061701, [arXiv:0901.0481](#) [[hep-ph](#)].
- [15] B. Herrmann, M. Klasen, and K. Kovarik, “SUSY-QCD effects on neutralino dark matter annihilation beyond scalar or gaugino mass unification,” *Phys. Rev.* **D80** (2009) 085025, [arXiv:0907.0030](#) [[hep-ph](#)].
- [16] N. Baro, F. Boudjema, and A. Semenov, “Full one-loop corrections to the relic density in the MSSM: A few examples,” *Phys. Lett.* **B660** (2008) 550–560, [arXiv:0710.1821](#) [[hep-ph](#)].
- [17] N. Baro, F. Boudjema, G. Chalons, and S. Hao, “Relic density at one-loop with gauge boson pair production,” *Phys.Rev.* **D81** (2010) 015005, [arXiv:0910.3293](#) [[hep-ph](#)].
- [18] F. Boudjema, G. D. La Rochelle, and S. Kulkarni, “One-loop corrections, uncertainties and approximations in neutralino annihilations: Examples,” [arXiv:1108.4291](#) [[hep-ph](#)].
- [19] J. Hisano, S. Matsumoto, and M. M. Nojiri, “Explosive dark matter annihilation,” *Phys.Rev.Lett.* **92** (2004) 031303, [arXiv:hep-ph/0307216](#) [[hep-ph](#)].
- [20] J. Hisano, S. Matsumoto, M. M. Nojiri, and O. Saito, “Non-perturbative effect on dark matter annihilation and gamma ray signature from galactic center,” *Phys.Rev.* **D71** (2005) 063528, [arXiv:hep-ph/0412403](#) [[hep-ph](#)].
- [21] N. Arkani-Hamed, D. P. Finkbeiner, T. R. Slatyer, and N. Weiner, “A Theory of Dark Matter,” *Phys.Rev.* **D79** (2009) 015014, [arXiv:0810.0713](#) [[hep-ph](#)].
- [22] R. Iengo, “Sommerfeld enhancement: General results from field theory diagrams,” *JHEP* **0905** (2009) 024, [arXiv:0902.0688](#) [[hep-ph](#)].
- [23] M. Drees, J. M. Kim, and K. I. Nagao, “Potentially Large One-loop Corrections to WIMP Annihilation,” *Phys. Rev.* **D81** (2010) 105004, [arXiv:0911.3795](#) [[hep-ph](#)].

- [24] A. Hryczuk, R. Iengo, and P. Ullio, “Relic densities including Sommerfeld enhancements in the MSSM,” *JHEP* **1103** (2011) 069, [arXiv:1010.2172 \[hep-ph\]](#).
- [25] A. Hryczuk and R. Iengo, “The one-loop and Sommerfeld electroweak corrections to the Wino dark matter annihilation,” *JHEP* **1201** (2012) 163, [arXiv:1111.2916 \[hep-ph\]](#).
- [26] H.-C. Cheng, J. L. Feng, and N. Polonsky, “Super-oblique corrections and non-decoupling of supersymmetry breaking,” *Phys. Rev.* **D56** (1997) 6875–6884, [arXiv:hep-ph/9706438](#).
- [27] E. Katz, L. Randall, and S.-f. Su, “Supersymmetric partners of oblique corrections,” *Nucl. Phys.* **B536** (1998) 3–28, [arXiv:hep-ph/9801416](#).
- [28] K.-i. Hikasa and Y. Nakamura, “Soft breaking correction to hard supersymmetric relations: QCD corrections to squark decay,” *Z.Phys.* **C70** (1996) 139–144, [arXiv:hep-ph/9501382 \[hep-ph\]](#).
- [29] H.-C. Cheng, J. L. Feng, and N. Polonsky, “Signatures of multi - TeV scale particles in supersymmetric theories,” *Phys.Rev.* **D57** (1998) 152–169, [arXiv:hep-ph/9706476 \[hep-ph\]](#).
- [30] M. M. Nojiri, D. M. Pierce, and Y. Yamada, “Slepton production as a probe of the squark mass scale,” *Phys. Rev.* **D57** (1998) 1539–1552, [arXiv:hep-ph/9707244](#).
- [31] S. Kiyoura, M. M. Nojiri, D. M. Pierce, and Y. Yamada, “Radiative corrections to a supersymmetric relation: A new approach,” *Phys. Rev.* **D58** (1998) 075002, [arXiv:hep-ph/9803210](#).
- [32] J. Guasch, W. Hollik, and J. Sola, “Fermionic decays of sfermions: A complete discussion at one-loop order,” *JHEP* **10** (2002) 040, [arXiv:hep-ph/0207364](#).
- [33] M. Drees, W. Hollik, and Q. Xu, “One-loop calculations of the decay of the next-to-lightest neutralino in the MSSM,” *JHEP* **0702** (2007) 032, [arXiv:hep-ph/0610267 \[hep-ph\]](#).
- [34] A. Chatterjee, M. Drees, S. Kulkarni, and Q. Xu, “On the On-Shell Renormalization of the Chargino and Neutralino Masses in the MSSM,” *Phys. Rev.* **D85** (2011) 075013, [arXiv:1107.5218 \[hep-ph\]](#).
- [35] T. Fritzsche and W. Hollik, “Complete one-loop corrections to the mass spectrum of charginos and neutralinos in the MSSM,” *Eur. Phys. J.* **C24** (2002) 619–629, [arXiv:hep-ph/0203159](#).
- [36] G. Belanger, F. Boudjema, A. Pukhov, and A. Semenov, “Dark matter direct detection rate in a generic model with micrOMEGAs2.1,” *Comput. Phys. Commun.* **180** (2009) 747–767, [arXiv:0803.2360 \[hep-ph\]](#).
- [37] A. Djouadi, J.-L. Kneur, and G. Moultaka, “SuSpect: A Fortran code for the supersymmetric and Higgs particle spectrum in the MSSM,” *Comput. Phys. Commun.* **176** (2007) 426–455, [arXiv:hep-ph/0211331](#).
- [38] P. Z. Skands, B. Allanach, H. Baer, C. Balazs, G. Belanger, *et al.*, “SUSY Les Houches accord: Interfacing SUSY spectrum calculators, decay packages, and event generators,” *JHEP* **0407** (2004) 036, [arXiv:hep-ph/0311123 \[hep-ph\]](#).

- [39] T. Hahn, “Generating Feynman diagrams and amplitudes with FeynArts 3,” *Comput. Phys. Commun.* **140** (2001) 418–431, [arXiv:hep-ph/0012260](#).
- [40] T. Hahn and C. Schappacher, “The implementation of the minimal supersymmetric standard model in FeynArts and FormCalc,” *Comput. Phys. Commun.* **143** (2002) 54–68, [arXiv:hep-ph/0105349](#).
- [41] T. Hahn, “A Mathematica interface for FormCalc-generated code,” *Comput. Phys. Commun.* **178** (2008) 217–221, [arXiv:hep-ph/0611273](#) [hep-ph].
- [42] T. Hahn and M. Perez-Victoria, “Automatized one-loop calculations in four and D dimensions,” *Comput. Phys. Commun.* **118** (1999) 153–165, [arXiv:hep-ph/9807565](#).
- [43] F. del Aguila, A. Culatti, R. Munoz Tapia, and M. Perez-Victoria, “Techniques for one-loop calculations in constrained differential renormalization,” *Nucl. Phys.* **B537** (1999) 561–585, [arXiv:hep-ph/9806451](#).
- [44] W. Siegel, “Supersymmetric Dimensional Regularization via Dimensional Reduction,” *Phys. Lett.* **B84** (1979) 193.
- [45] A. Belyaev, N. D. Christensen, and A. Pukhov, “CalcHEP 3.4 for collider physics within and beyond the Standard Model,” [arXiv:1207.6082](#) [hep-ph].
- [46] K. Nakamura *et al.*, “Review of particle physics,” *J. Phys.* **G37** (2010) 075021.
- [47] G. Gamberini, G. Ridolfi, and F. Zwirner, “On Radiative Gauge Symmetry Breaking in the Minimal Supersymmetric Model,” *Nucl. Phys.* **B331** (1990) 331–349.
- [48] B. de Carlos and J. A. Casas, “One loop analysis of the electroweak breaking in supersymmetric models and the fine tuning problem,” *Phys. Lett.* **B309** (1993) 320–328, [arXiv:hep-ph/9303291](#).
- [49] M. Consoli, W. Hollik, and F. Jegerlehner, “Electroweak radiative corrections for  $Z$  physics,”.
- [50] A. Sirlin, “Role of  $\sin^2 \theta_W(m_Z)$  at the  $Z^0$  Peak,” *Phys. Lett.* **B232** (1989) 123.
- [51] R. J. Scherrer and M. S. Turner, “On the Relic, Cosmic Abundance of Stable Weakly Interacting Massive Particles,” *Phys. Rev.* **D33** (1986) 1585.
- [52] D. M. Pierce, J. A. Bagger, K. T. Matchev, and R.-j. Zhang, “Precision corrections in the minimal supersymmetric standard model,” *Nucl. Phys.* **B491** (1997) 3–67, [arXiv:hep-ph/9606211](#).
- [53] K. Griest and D. Seckel, “Three exceptions in the calculation of relic abundances,” *Phys. Rev.* **D43** (1991) 3191–3203.
- [54] J. R. Ellis, T. Falk, and K. A. Olive, “Neutralino - Stau coannihilation and the cosmological upper limit on the mass of the lightest supersymmetric particle,” *Phys. Lett.* **B444** (1998) 367–372, [arXiv:hep-ph/9810360](#) [hep-ph].
- [55] M. Drees, M. M. Nojiri, D. Roy, and Y. Yamada, “Light Higgsino dark matter,” *Phys. Rev.* **D56** (1997) 276–290, [arXiv:hep-ph/9701219](#) [hep-ph].
- [56] W. J. Marciano and A. Sirlin, “Radiative Corrections to Neutrino Induced Neutral Current Phenomena in the  $SU(2)_L \times U(1)$  Theory,” *Phys. Rev.* **D22** (1980) 2695.

- [57] A. Denner, “Techniques for calculation of electroweak radiative corrections at the one loop level and results for W physics at LEP-200,” *Fortschr. Phys.* **41** (1993) 307–420, [arXiv:0709.1075 \[hep-ph\]](#).
- [58] M. Steinhauser, “Leptonic contribution to the effective electromagnetic coupling constant up to three loops,” *Phys.Lett.* **B429** (1998) 158–161, [arXiv:hep-ph/9803313 \[hep-ph\]](#).
- [59] K. Hagiwara, R. Liao, A. D. Martin, D. Nomura, and T. Teubner, “ $(g - 2)_\mu$  and  $\alpha(M_Z^2)$  re-evaluated using new precise data,” *J.Phys.G* **G38** (2011) 085003, [arXiv:1105.3149 \[hep-ph\]](#).
- [60] P. H. Chankowski, S. Pokorski, and J. Rosiek, “Complete on-shell renormalization scheme for the minimal supersymmetric Higgs sector,” *Nucl. Phys.* **B423** (1994) 437–496, [arXiv:hep-ph/9303309](#).
- [61] A. Dabelstein, “The One loop renormalization of the MSSM Higgs sector and its application to the neutral scalar Higgs masses,” *Z. Phys.* **C67** (1995) 495–512, [arXiv:hep-ph/9409375](#).
- [62] A. Dabelstein, “Fermionic decays of neutral MSSM Higgs bosons at the one loop level,” *Nucl. Phys.* **B456** (1995) 25–56, [arXiv:hep-ph/9503443](#).
- [63] N. Baro and F. Boudjema, “Automatised full one-loop renormalisation of the MSSM II: The chargino-neutralino sector, the sfermion sector and some applications,” *Phys. Rev.* **D80** (2009) 076010, [arXiv:0906.1665 \[hep-ph\]](#).